Doctoral Thesis in Industrial Engineering

------XXVI cycle

Modulation of Drug Release from Polymeric Carriers and Systems

Qiang Qian

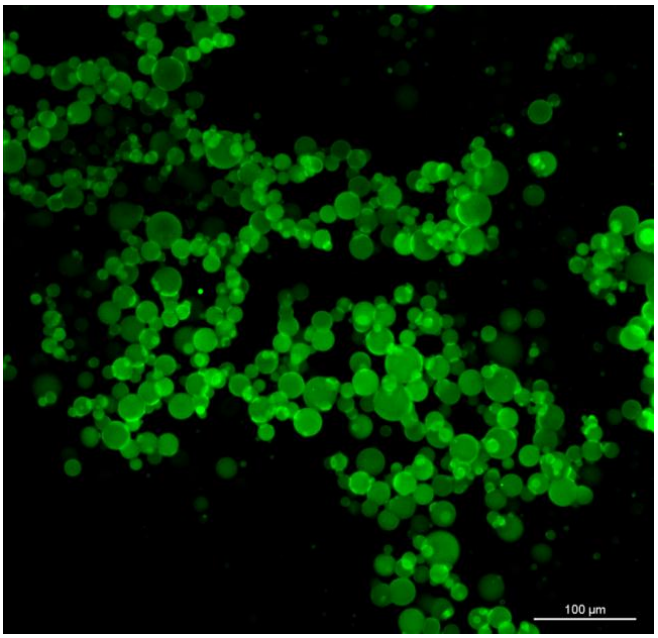

University of Trento
Department of Industrial Engineering
BIOtech research center

Tutor: Prof. Claudio Migliaresi
Advisor: Dr. Walter Bonani

Date of the graduation
09.10.2014

Acknowledgments

I would like to thank all of them that have contributed to the accomplishment of this work during my PhD course.

First of all, I would like to express my deep gratitude to my supervisor, Prof. Claudio Migliaresi, who gave me this opportunity to have this memorable study experience in the BIOtech group. He always gave his scientific support, patience and encouragement to me during my study in Trento. In the occasion of the successful completion of this thesis, the author would like to express the sincere respect and heartfelt thanks to Prof. Claudio Migliaresi.

I am indebted to Walter Bonani, my “little tutor”, who taught me many skills and gave me many valuable discussions and patient guidance on my experiments, papers and thesis. His rigorous attitude and careful spirit on science will influence my whole life.

I also appreciate Prof. Antonella Motta and Prof. Devid Maniglio, who gave me so many kind helps, both in my study and in my daily life. Their warmhearted help made a lonely foreigner feel warm and less lonely when I first arrived in Trento.

The BIOtech group is like a big and warm family. I acknowledge all the people of the BIOtech group and all the time with all of you, from the study, the picnics, and Christmas lunches. In particular, I am indebted to Christian Lorandi, Luca Gasperini, Mariangela Fedel, Cristina Foss, Luca Dalbosco, Filippo Benetti, Matteo Stoppato, Eleonora Carletti, Lucia Verin, Wei Sun and Lorenzo Moschini. Although most of them have already graduated, the memory is still there.

A special thank goes to the project of “Bridge the Gap” for the invaluable help and financial supports.

Last but not least, I want to thank my wife, parents and my little daughter for their support and encouragement.

Contents

List of figures

Abstract

Controlled drug delivery systems, which are intended to deliver drugs at predetermined rates for predefined periods of time, have been used to overcome the shortcomings of conventional drug formulations.

Injectable drug-loaded matrices and controlled release technology offer numerous advantages compared to conventional dosage. However, one of the greatest challenges in applying this system to the clinical phase is the relatively large initial burst release.

To reduce this effect of large initial burst release, a new drug delivery system was fabricated in this thesis. Both alginate and gelatin are biocompatible nature polymers and have been largely used as biomaterials for long time. By cross-linking alginate solution carrying drug-loaded uncross-linked gelatin microbeads, the initial burst release was reduced significantly, compared with drug directly releasing from gelatin or cross-linked alginate matrix.

Firstly, a series of gelatin microbeads were prepared in a water-in-oil (W/O) emulsion by a traditional emulsification method. The effects of the concentration of gelatin solution, volumetric ratio of water-to-oil phase, stirring speed and emulsifying time on the particle size and dispersity of gelatin microbeads were studied.

Secondly, drug-loaded gelatin microbeads were encapsulated into the cross-linked sodium alginate macro-beads. The release behavior of drug-loaded gelatin microbeads encapsulated within cross-linked alginate gel was characterized both at room temperature and 37℃ and compared with the release from gelatin microbeads and cross-linked alginate gel alone. This system represents a promise for the development of novel and versatile injectable drug delivery systems.

Thirdly, a dual-drug delivery system was fabricated by encapsulating drug-loaded gelatin microbeads into the mixture of cross-linkable sodium alginate and another drug. The effects of preparation methods of drug-loaded gelatin microbeads and ratio between gelatin microbeads and alginate on drug release behaviors of both drugs were studied. This system shows a significant potential in dual drug delivery field due to the synergistic effect between gelatin and alginate.

Additionally, combination of multi-drugs in one system has been revealed as a promising application in the drug delivery systems. Therefore, in the fifth chapter of this thesis, an idea for the multi-drug delivery system was simply demonstrated. Rods of gelatin gels loaded with different drugs were separated by the agarose gel in a polycarbonate

tube. The effects of the length of agarose gel and temperature on the drug release profiles were investigated. The results suggested the feasibility to employ this idea to the practical applications.

Chapter 1

Introduction

1.1 Drug Delivery Systems

There are some shortcomings in the clinical applications of traditional medicines and formulations, such as low effectiveness of the drugs, high side effects and the frequent needs of medication to maintain efficacy [1].

Drug delivery systems (DDS) are the systems to deliver drugs to the target sites of pharmacological actions. In detail, DDSs refer to the drug carriers, composed primarily of lipids and/or polymers, approaches, formulations, technologies, and systems to deliver the drugs in the body as needed to safely achieve the required therapeutic effect. Technologies employed include those concerning drug preparation, route of administration, site targeting, metabolism, and toxicity [2-4].

DDS is designed to efficiently target within the body as the drug reservoirs for sustained drug release, to decrease the antigenicity and increase the bio-distribution of the loaded drugs, or to reduce the toxicity of high drug loading; whatever the case may be, it is mainly concerned with dosage form, route of administration and duration of drug presence. Drug delivery is often approached via a drug's chemical formulation, but it may also involve medical devices or drug-device combination products [5].

Design, research and production of efficient drug delivery systems are of significant importance for the improvement of medicine and healthcare. Since the first FDA approval of drug delivery system (DDS) in 1990, more than 10 DDS are now commercially available to treat diverse diseases ranging from cancer to fungal infection and to muscular degeneration (Figure. 1.1) [6].

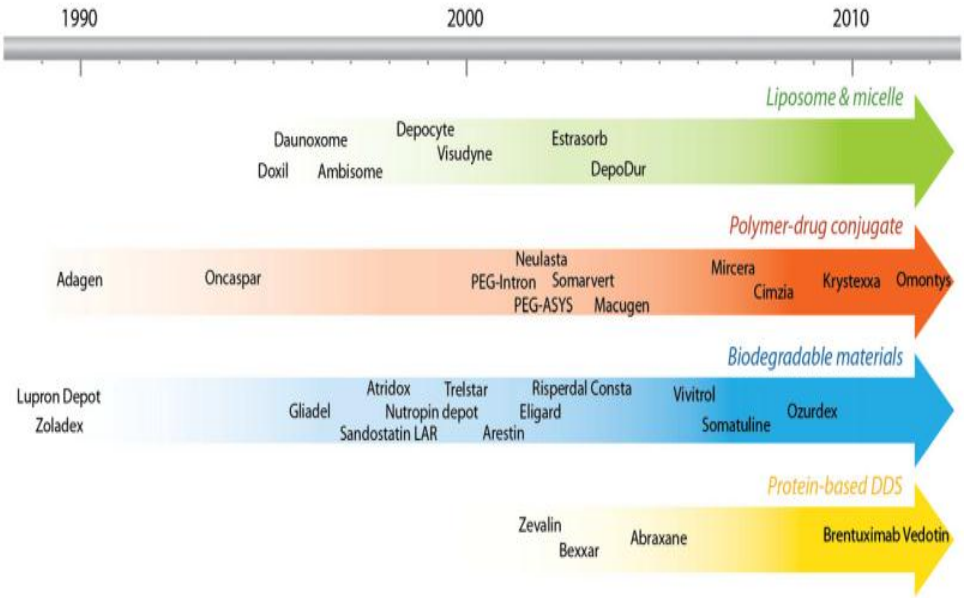

Figure 1.1: Timeline showing FDA approved DDS in the market [6].

With the development of therapeutic efficacy, more and more patients have relieved suffering and prolonged life profited from DDS. At the same time, drug delivery systems have also changed the economics of drug production. As a new product, incorporating an existing drug into a suitable drug delivery system not only improves drug's performance but also reduce patents' suffering and cost. According to the statistics, the average cost and time required to develop a new DDS is approximately $20–50 million and 3–4 years, while it is significantly higher to develop a new drug (approximately $500 million and over 10 years) [7]. It is not surprising that the annual worldwide market for advanced and controlled drug release system has grown dramatically [8], especially in the US market [9].

Many of the pharmacological properties of conventional drugs can be improved through the use of drug delivery systems, Table 1.1 [4] gives examples of problems exhibited by free drugs that can be ameliorated by the use of DDS.

With the help of drug delivery systems, drug release profiles could be modified, as well as absorption and distribution of the drugs, which improve drugs' efficiency and safety. Moreover, DDS increase patients' convenience and compliance. Most common routes of administration of drugs include the preferred non-invasive peroral (through the mouth), topical (skin), transmucosal (nasal, buccal/sublingual, vaginal, ocular and rectal) and inhalation routes [10]. However, with these common routes, a big problem is emerged: many drugs such as peptide, antibody and vaccine cannot be delivered and adsorbed into the systemic circulation efficiently and properly. The primary reasons come to easily enzymatic degradation, improper molecular size and charge-based problems. Therefore, many protein and peptide drugs have to be delivered by injection or a nano-needle array. For

example, many protein-based insulin and immunizations are often delivered by injection.

Table 1.1 Non-ideal properties and problems of drugs in common routes and their therapeutic effects of DDS [4].

Problem	Implication	Effect of DDS
Poor solubility	A convenient pharmaceutical format is difficult to achieve, as hydrophobic drugs may precipitate in aqueous media. Toxicities are associated with the use of excipients such as Cremphor (the solubilizer for paclitaxel in Taxol).	DDS such lipid micelles or liposomes provide both hydrophilic and hydrophobic environments, enhancing drug solubility.
Tissue damage on extravasation	Inadvertent extravasation of cytotoxic drugs leads to tissue damage, e.g., tissue necrosis with free doxorubicin.	Regulated drug release from the DDS can reduce or eliminate tissue damage on accidental extravasation.
Rapid breakdown of the drug in vivo	Loss of activity of the drug follows administration, e.g., loss of activity of camptothecins at physiological Ph.	DDS protects the drug from premature degradation and functions as a sustained release system. Lower doses of drug are required.

Unfavorable pharmacokinetics	Drug is cleared too rapidly, by the kidney, for example, requiring high doses or continuous infusion.	DDS can substantially alter the PK of the drug and reduce clearance. Rapid renal clearance of small molecules is avoided.
Poor bio-distribution	Drugs that have widespread distribution in the body can affect normal tissues, resulting in dose-limiting side effects, such as the cardiac toxicity of doxorubicin.	The particulate nature of DDS lowers the volume of distribution and helps to reduce side effects in sensitive non-target tissue.
Lack of selectivity for target tissues	Distribution of the drug to normal tissues leads to side effects that restrict the amount of drug that can be administered. Low concentrations of drugs in target tissues will result in suboptimal therapeutic effects.	DDS can increase drug concentrations in diseased tissues such as tumors by the EPR effect. Ligand-mediated targeting of the DDS can further improve drug specificity.

As shown in Figure 1.2, traditional mechanisms of drug delivery for controlling the rate of drug release from polymeric drug delivery systems can be summarized as the following four types [11-15]: (1) diffusion-controlled systems, where the release rate is determined by diffusion coefficient of the drug in the current conditions [16], such as PEVAC; (2)

swelling-controlled systems, where the release rate of drug is based on the water swelling rate of the delivery system, swelling increases the flexibility of the polymer and makes larger pores, resulting in better drug mobility [17], such as PVA, PHEMA; (3) degradation-controlled systems, where the drug release rate depends on the level of chemical or physical degradation of the drug delivery matrix, it could be surface degradation or bulk degradation [18], such as PLGA, PCL; (4) external stimulus-controlled systems, where stimulus-controlled systems release therapeutic factors upon activation by a stimulus or multiple stimuli, leading to a physical or chemical change in the delivery system, these stimuli could be physical (e.g., pH, temperature) or chemical (e.g., the presence of glucose) [5], such as PNIPAM, PDMAEMA.

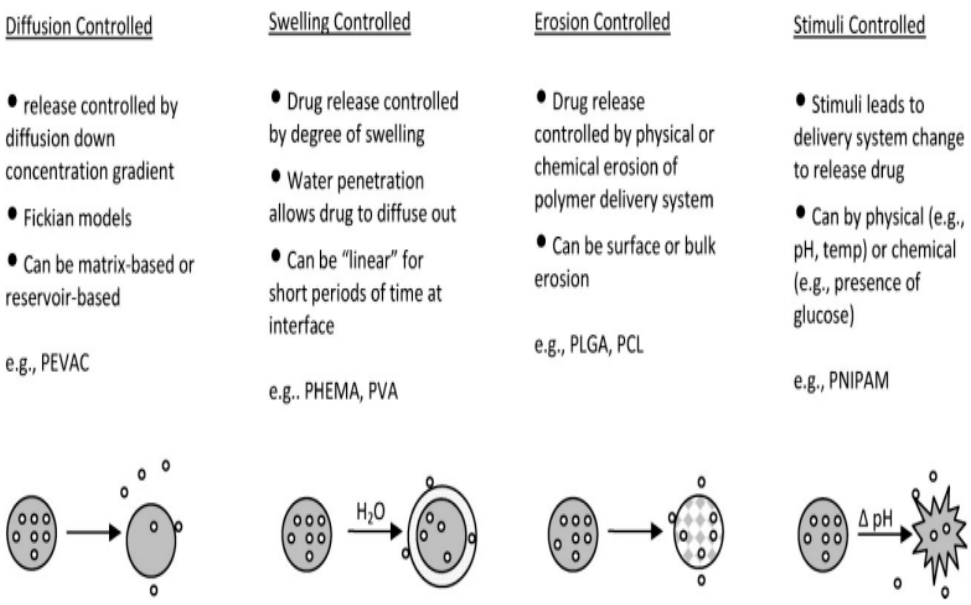

Figure 1.2 : Summary of four traditional mechanisms of drug delivery systems: diffusion-controlled, swelling-controlled, degradation-controlled, and stimuli-controlled systems [11].

Among the four common mechanisms, initial drug burst was inevitable. The novel concept of using chemical affinity in drug delivery systems can reduce initial burst and control drug release availably. As defined, affinity is the tendency of a molecule to associate with another molecule. It may come from many chemical or physical interactions, such as covalent bond, charged interaction, hydrogen bonding or van der Waals forces. It has been reported that stable polyion complex can be formed by the electrostatical interaction between two polyelectrolytes with opposite charges. By the interaction or affinity between drug and polymeric matrices, drug loading and release could be controlled [11, 19].

Recently drug delivery system includes oral drug delivery system, transdermal drug delivery system, mucosal drug delivery system, targeted drug delivery system, cell micro-encapsulated drug delivery system and microfabricated drug delivery system.

The main efforts in the field of drug delivery include the development of targeted delivery and sustained release formulations. To be specific, the drug would be only active in the target area of the body (for example, in cancerous tissues) in the targeted DDS and the drug would be released over a period of time in a controlled manner in the sustained DDS. In order to realize the efficiency of targeted delivery, the designed system must avoid the body's immune mechanisms and then manage to deliver the drugs to its intended site of action. Types of sustained release formulations include liposomes, drug loaded biodegradable microspheres and drug polymer conjugates.

Innovation and development in materials have initially driven the progress of DDS. Various kinds of carriers have been created, like biodegradable, biocompatible, targeting, stimulus-responsive and injectable

materials. Nanotechnology has also contributed much to the development of DDS in the past decade. Since then when it was found that size and shape of nanoparticles (NPs) could help navigate biological carriers, the application of nanofabrication technologies has motivated to develop more effective particulate DDS, both top–down and bottom–up. As reported, the size of NPs regulates their bio-distribution. Particles less than 20 nm will be cleared from circulation via reticuloendothelial system (RES) within a few hours when injected intravenously, whereas larger ones will be trapped in the liver and the spleen within minutes [20, 21]. In a study of Kataoka and his colleagues, the results showed that polymeric micelles only less than 30 nm could effectively penetrate poorly permeable pancreatic tumor cells [22]. Fabricating techniques such as nano-precipitation, emulsion-based phase inversion, microfluidics-based self-assembly, layer-by-layer synthesis, and nano-imprinting have been used to generate particulate DDS to deliver a wide range of drugs. With the full understanding of the potential of particulate DDS in required size and shape, nano-fabrication and nano-manufacturing will play a more and more prominent role in the future.

As the carriers of drug delivery systems, they could be these traditional biodegradable polymers, such as poly (lactic acid) (PLA), poly (glycol acid) (PGA) and their copolymers, poly (lactide-co-glycolide) (PLGA), they are the most widely used for the development of drug delivery system because of their biodegradability, biocompatibility and ease of processing [23, 24]; they could be block copolymers, such as poly (propylene oxide)-poly (ethylene oxide)- poly(propylene oxide) (PPO-PEO-PPO) (Pluronic) triblock copolymer, developed by Kabanov et al., they have attracted the thoughts of researchers since the early days of drug delivery because of their remarkable chemical flexibility. Depending on the choice of building blocks,

they could assemble to nanostructures in the form of micelles, electrostatic complexes, or polymersomes [25]; they could be polymer drug conjugates, conjugation to a polymeric carrier via a liable linker presents another attractive approach to alter and optimize the pharmacokinetics of therapeutic agents [6]; they could be natural polymers derived from biological systems including protein, DNA, and polysaccharides, they are biocompatible and biodegradable, moreover, they possess low toxicity and potentially favorable pharmacokinetics in the circulation [6]; they also could be recombinant protein-based drug carriers.

1.2 Gelatin

Nowadays, gelatin is utilized in practically all areas of modern life. However, interest in gelatin is not just restricted to classical applications; this natural product has numerous other application possibilities. New applications in health care and in specialized technical areas will result in gelatin and gelatin hydrolysates becoming a focal point of concern for a much wider pubic [26].

The first known gelatin by boiling animal tissues to use as glue should date back to about 8000 years ago. The revolution in the use of gelatin for biomedical applications occurred in 1833 when gelatin capsules were first fabricated to encapsulate drugs to prevent drugs from heat, humidity and to make drugs taste no longer bitter. In the 20^{th} century, the application of gelatin in medical field exploded [26].

Gelatin is a mixture of protein, which is easily available through native collagen hydrolysis processing of animal skin (it would be possible to use

also bones, but it is more difficult; for economical and practical reasons, skin is usually preferred), either by partial acid or alkaline hydrolysis at a moderate temperature; the content of protein ranges from 85% to 92%, the remnant consists of salts and moisture remained after drying [26-28].

By controlling type and intensity of the hydrolysis, it is possible to control the molecular weight distribution. Gelatin hydrolyzed with alkaline treatment (type B) shows a narrower distribution, while type A gelatin has a broader distribution. Molecular weight will affect viscosity and gelling power. Both of them are increased by the increase in the molecular weight. The gel strength is the most important quality parameter for gelatin. The analytical measure of gelling power is the Bloom value, which is the weight required for a specified plunger to depress the surface of a standard, thermostatted gel to a defined depth under standard conditions.

Gelatin undergoes a sol-gel phase transition at a temperature close to 35 ℃, which can slightly vary due to gel strength, concentration and thermal history of the material [26, 29]. The kinetics of gel formation of gelatin can be explained by the formation of intermolecular hydrogen bonds (Figure 1.3). When gelatin solution is cooled down, the mobile molecules aggregate to small clusters; these continuously grow and subsequently form the gel [26]. Usually the gelation temperature of gelatin is 5 ℃ below the melting temperature. The unique ability to react with heat (undergo gel-to-sol transition at body temperature) has made animal-derived gelatin extensively used as gelling agents in the modern food, biomaterial, medical and pharmaceutical industry [1, 26, 30-33]. However, uncross-linked gelatin hydrogels tend to be in liquid phase at body temperature and this is usually a limiting factor for *in vivo* applications. Therefore, chemically cross-linked gelatin has been used as a substitution widely for tissue engineered scaffold

and as carrier for drugs, gene therapeutic entities and cells [32, 34-38], although it is non-degradable and loses the ability for the sol-gel transition *in vivo*.

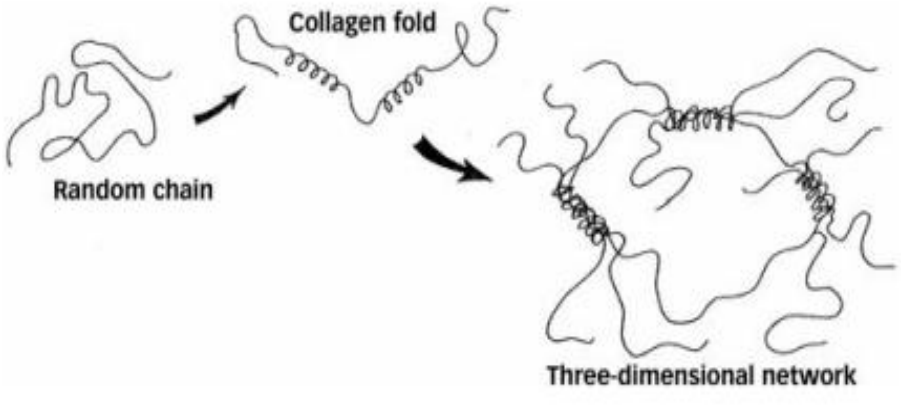

Figure 1.3: Model of gel formation (from sol to gel upon cooling) [26]

Drug delivery systems based on this polymer are known to be biocompatible, biodegradable without toxic by-products and characterized by low immugenicity. Gelatin is a polyampholyte having both cationic and anionic groups along with hydrophilic groups. The electrical nature of gelatin, which can be changed by the hydrolysis processing method--acid treatment for basic gelatin; alkaline treatment for acid gelatin, has endowed it another unique advantage as a drug carrier [1, 31-33]. Thanks to the duplicity of gelatin, different type of gelatin (type A: basic; type B: acidic) would be chosen[39, 40] to meet the demand of immediate [41] or sustained [31, 40] drug release, depending on the alkalinity or acidity of drug and application. Furthermore, conjugates formed by gelatin and drug have many advantages, including biodegradability, low antigenicity with the potential to

overcome immune problems and reducing the toxicity of high drug loading [42, 43].

1.3 Alginate

Commercial alginates are mainly extracted from three kinds of native brown seaweed: Laminaria hyperborean, Ascophyllum nodosum, and Macrocystis pyrifera [44]. Alginate, the primary polysaccharide in the these seaweed, is found in the intracellular matrix. The native alginate is mainly present as an insoluble Ca^{2+} cross-linked gel [45].

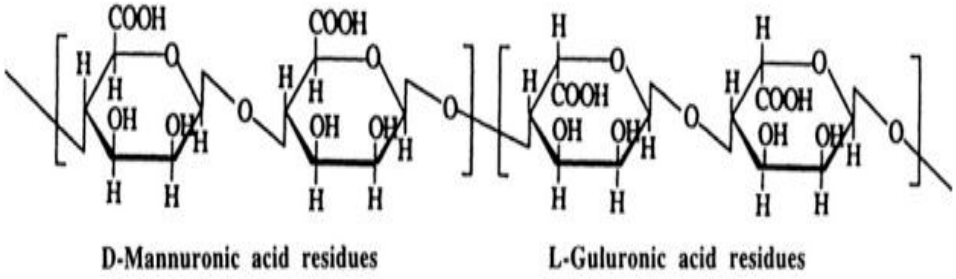

Figure 1.4: Structure of alginate [46]

Alginate is a family of linear unbranched polysaccharides which contain varying amounts of 1, 4'-linked β-D-mannuronic acid (M) and α-L-guluronic acid (G) residues, as shown in Figure 1.4 [46]. Cross-linking of alginate gel can take place easily in mild conditions when the solution of sodium alginate meets divalent cations, such as Ca^{2+}, Ba^{2+} or Sr^{2+}, these cations cooperatively interact with blocks of G monomers forming ionic inter-chain bridges (characteristic egg-box structure) and causing the gelification of the alginate solution [47-49], the schematic representation is

shown in Figure 1.5. Among these cations, Ba^{2+} or Sr^{2+} ions produce stronger alginate gels than Ca^{2+} [49-51]. However, monovalent cations and Mg^{2+} ions do not induce gelation, other divalent cations also can cross-link alginate but their use is limited due to the toxicity.

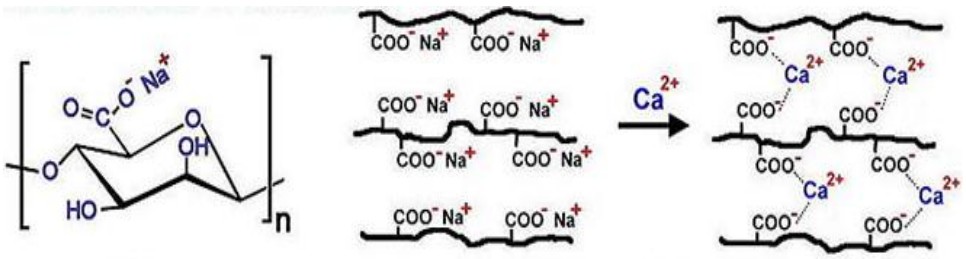

Figure 1.5: Schematic representations of the poly-L-guluronate sequences of alginate cross-linked by calcium ions [49].

Alginate has been widely used in food and beverage industries as well as tablet manufacture for long time [52]. Due to the large availability in nature, the mildness of gelation conditions, limited toxicity, great biocompatibility, low immunogenicity, and low cost [47, 49, 52, 53], alginate has been widely proposed as a potential biopolymer for drug stabilization, tissue engineering, and controlled-release systems, as well as for cells encapsulation techniques [54-58].

Recently alginate gains increasing interests in its applications as scaffolds of injectable, self-cross-linkable and long-term degradable hydrogels. Development on injectable auto-forming alginate gel by encapsulating calcium phosphate or calcium-rich alginate microbeads into alginate solution as well as blending oxidized alginate with gelatin solution has been reported[13, 41, 59-61]. Alginate solutions also have been shown to form

gels in situ when placed on the surface of the eye [62]. Ito et al.[61] reported that cross-linking of alginate could occur spontaneously once injected into a living body because of divalent cations in the organism. In addition, although cross-linked alginate is non-biodegradable, degradation can occur by removal of the cross-linking ions[49], for instance, alginate gels will degrade in 0.1 M phosphate buffer solution[63]. Therefore, since the exit of HCO_3^- and HPO_4^{2-} in the human body fluid[61], the degradation of alginate gels can also take place in vivo. However, majority of them suffer the problem on fast release of encapsulated drugs which limits its application as the matrix of drug delivery system. To prolong the duration of drug release, it is a feasible way to immobilize drugs to charged polymer carriers by electrostatically interaction to form a polyion complex [64] or embed drug-loaded microbeads in polymeric matrix. Varied microbeads, micelle and beads were developed to trap drugs and delivery the drugs with assistance of polymeric matrix [65-69], and for the polyion complexation for sustained release, it is necessarily bio-safe and biodegradable.

1.4 Objectives

The aim of this research is to develop an uncross-linked gelatin based composite to be used for drug delivery system or multi-drug delivery system. The composite should have the ability to control the rate of drug release as needed, no matter immediate release or sustained release. It also should have the following characteristic: non-toxicity, great biocompatibility, low immunogenicity, low cost and degradability in vivo. The scheme of my study was shown in Figure 1.6.

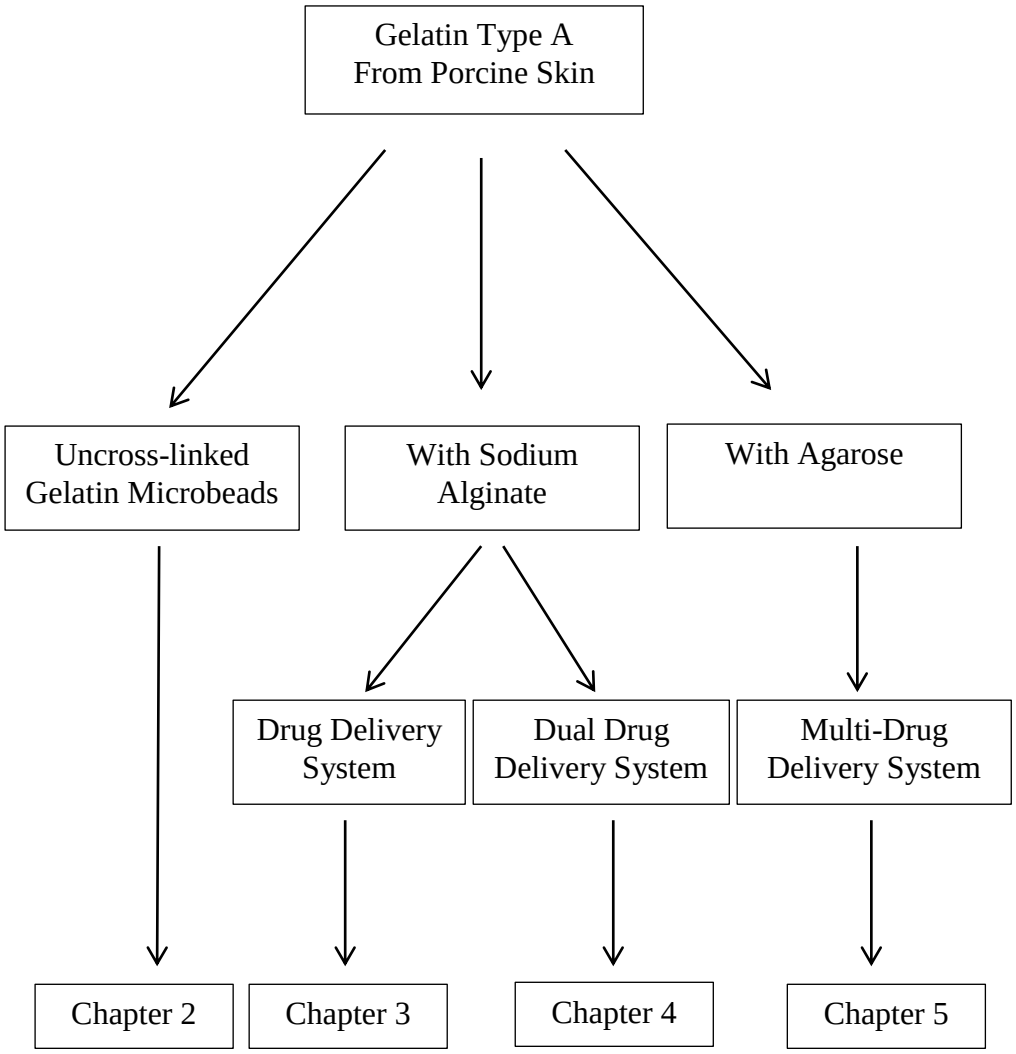

Figure 1.6: The scheme of the thesis.

Chapter 2

Preparation and characterization of gelatin microbeads

2.1 Introduction

In recent years the application of encapsulating micro-particles into drug delivery system has gained more and more attentions. Due to different kinds of drug needs, such as immediate release, sustained release of constant drug concentration for some time or targeting to specific cells or organs, drug delivery systems based on the particles have widely utilized in experimental therapeutics. For instance, antineoplastic drugs have been selectively targeted with antitumor agents to obtain higher drug concentration at the tumor site in real clinical application [70, 71] . As for the sustained release, the direct relationship between route of administration and particle size should be considered.

Microspheres with diameter in the range of 20-100 μm can be chosen for subcutaneous or intramuscular administration as sustained release depots. Smaller micro-particles have been considered for the treatment of infection and arthritis [72].

Embedding biodegradable particles into the formulation turns to be efficient to improve the therapeutic effect of various water soluble/insoluble medicinal drugs and bioactive molecules. In this way, absorption, bioavailability, intracellular penetration, solubility and retention time of drugs in the selected tissue are improved. The resulting formulation would reduce the risks of side effect and the cost of patients and protect the premature degradation and interaction with the biological environment [73-76].

Drugs or bioactive molecules related to some dreadful diseases like cancer, AIDS, diabetes, malaria and prion disease are successfully encapsulated into nano- or micro-particles to improve bioavailability, bioactivity and control delivery, some of them are already commercialized [77-81].

The size of the particles plays a significant role in the aspect of properties of the final product as well as potential applications during the drug release. Size also has a marked effect on particle distribution throughout the body. When delivered in vivo, large particles will tend to lodge in the injected tissues or small vessels [82], while smaller ones, especially nanoparticles, may circulate in the bloodstream or may be eliminated by white blood cells for a period of time determined by many elements, such as size and surface chemistry [83]. As for the ability to overcome the biological obstacles, nanoparticles can easily achieve this; while, for the microparticles, the only

two ways to cross the most barriers are injection and carrying by a particular cell type.

In this chapter, gelatin microbeads would be prepared under all kinds of conditions by emulsification and the optimal parameter would be selected to obtain the suitable drug-loaded gelatin microbeads.

2.2 Materials

Gelatin (gelatin type A, gel strength ~300 g Bloom, from porcine skin), soybean oil, nonionic surfactant sorbitane monooleate (Span® 80) and n-Hexane were purchased from Sigma-Aldrich (Milan, Italy). All the materials were used as received without further purification.

2.3 Methods

2.3.1 Preparation of gelatin solution

Different gelatin aqueous solutions were prepared by soaking gelatin powder in deionized water for 10 minutes, at room temperature, to allow gelatin swelling by absorbing a certain amount of liquid. The suspensions were then placed in a 40 ℃ bath for one hour and stirred every 20 minutes by using a vortex mixer until a clear gelatin solution was obtained.

2.3.2 Preparation of oily phase

Oily phase was a mixture of commercial soybean oil and Span® 80, prepared in a proportion of 20 mg of Span® 80 per 1 mL of soybean oil under mild stirring in a 40 ℃ water bath.

2.3.3 Preparation of gelatin microbeads

An emulsification-coacervation method was employed to prepare gelatin microbeads [84-87]. Briefly, a gelatin solution prepared as in section 2.3.1 was added dropwise into the oily phase prepared as in section 2.3.2 under continuous stirring in a 40 ℃ water bath to obtain a water-in-oil (W/O) emulsion. Different volume ratio between gelatin solution and oily phase was used. The effects of emulsifying time ranging from 2 to 15 min and stirring speed ranging from 200 to 1000 rpm on the W/O emulsion were also considered. After this stage, the emulsion was moved to an ice-bath and stirred for other 30 min at 200 rpm to complete the gelation of the gelatin microbeads inside the continuous oily phase. Oil was then removed with several washings in n-hexane and gelatin microbeads were placed in a vacuum drier overnight to remove hexane.

2.3.4 Characterization of gelatin microbeads

Gelatin microbeads obtained in the different conditions were imaged with optical microscope (Axiotech, Carl Zeiss, Germany). For particle size, at least 30 microbeads per image were measured and analyzed using ImageJ software (National Institutes of Health, Bethesda, MD, USA). All the data were presented as mean ± standard deviation. Statistical analysis was

performed using OriginPro software (OriginLab, Northampton, MA, USA) with significance level of $p < 0.05$.

2.4 Results and Discussion

2.4.1 Characterization of gelatin microbeads

Emulsification method has been widely applied to the preparation of micrometric beads for its outstanding advantages such as easy-controlling and mild-condition operation, which was first proposed by Tanaka.[88] In this study a plant-derived soybean oil was chosen as the oily phase for safety considerations because it is often difficult to completely remove the oil after microbeads preparation.[89]

Solid and water stable gelatin microbeads with homogenous size and spherical shape and narrow distribution were prepared by water-in-oil (W/O) emulsification method. The particle size of gelatin microbeads was strongly dependent on the different operational parameters used during preparation. In the present study, the influence of gelatin concentration, emulsifying speed, the ratio between gelatin solution and oily phase, and emulsifying time on particle size were investigated.

2.4.1.1 Effect of the concentration of gelatin solution on the size of gelatin microbeads

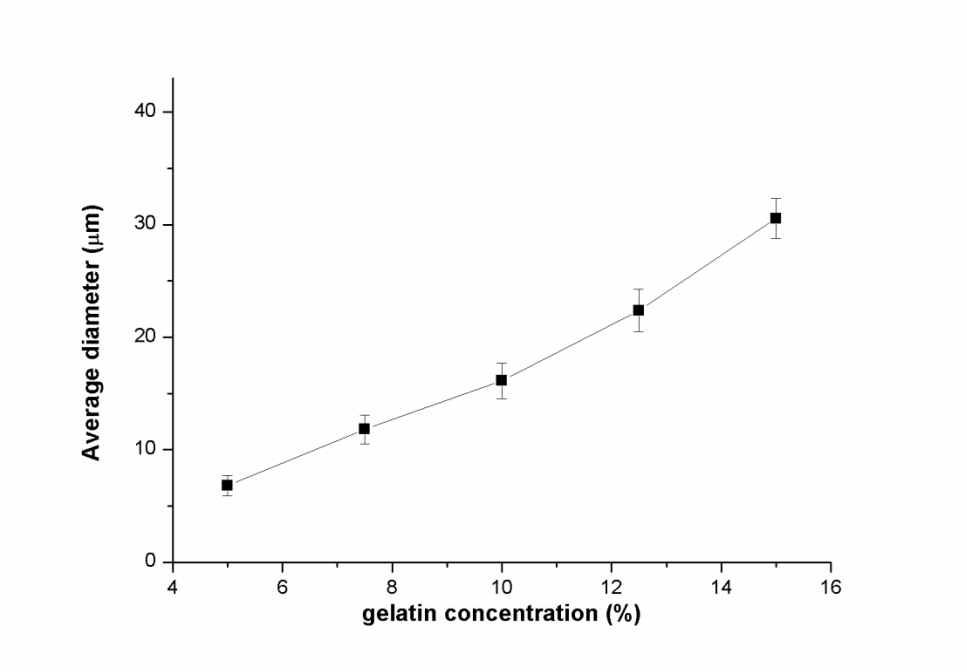

Figure 2.1 Average diameter of gelatin microbeads prepared from gelatin solution of different concentrations (ratio between water phase and oily phase: 1:5, stirring speed: 800 rpm and emulsifying time: 10 minutes)

The concentration of gelatin solution is one of the important parameters that influence the morphology and size of gelatin microbeads. When the concentration of gelatin solution is lower than 20 μg/mL, it is difficult for the gelatin solution to form the microbeads. For the water content in the drop of gelatin solution is too high, once the drop cools down to form the gel, the shape of particles obtained will be irregular after dehydration and the inner structure of the particles will be very loose. Therefore, it is not

proper to prepare gelatin microbeads by using low concentration gelatin solution.

In our case, five concentrations of 50 μg/mL, 75 μg/mL, 100 μg/mL, 125 μg/mL and 150 μg/mL (5%, 7.5%, 10%, 12.5%, 15% (w/v)) were chosen to obtain different gelatin microbeads for comparison by fixing the ratio of 1: 5 between gelatin solution and oily phase, stirring speed of 800 rpm and 10 min of emulsifying time.

As shown in Figure 2.1, the particle size of gelatin microbeads increased almost linearly from 6.8 ± 0.9 μm to 30.6 ± 1.8 μm with the concentration of gelatin solution ranging from 5% to 15%.

From Figure 2.2, it could be seen that when gelatin microbeads were prepared from low-concentration gelatin solution, the microbeads with smaller particle size had a strong tendency to agglomerate, which attributed to the high water content in the gelatin microbeads. During the stirring of preparation, it was easy to destroy the inner loose structure of gelatin microbeads, which would lead to the particles stick to each other.

With the increase of concentration of gelatin solution, the morphology and the dispersity of the gelatin microbeads would be improved significantly, the phenomenon of agglomeration would disappear, as shown from Figure 2.3.

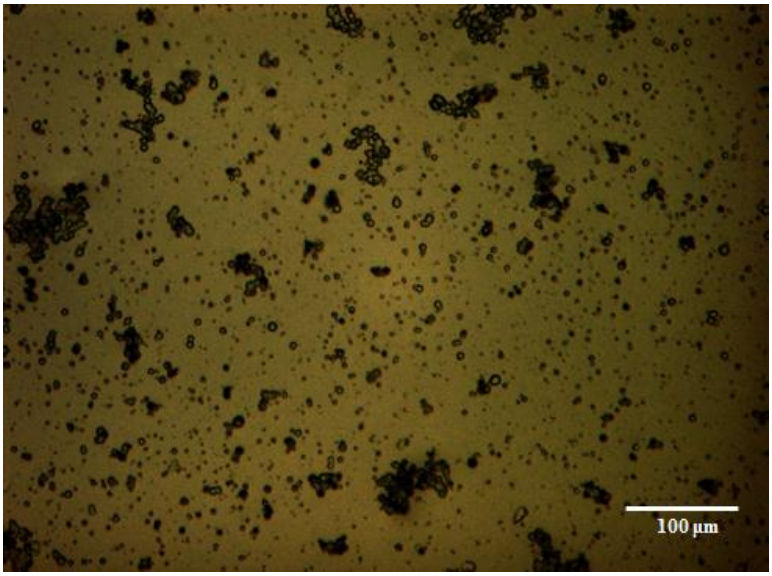

Figure 2.2. Optical image of gelatin microbeads in oily phase prepared from 50 µg/mL gelatin solution (ratio between water phase and oily phase: 1:5, stirring speed: 800 rpm and emulsifying time: 10 minutes)

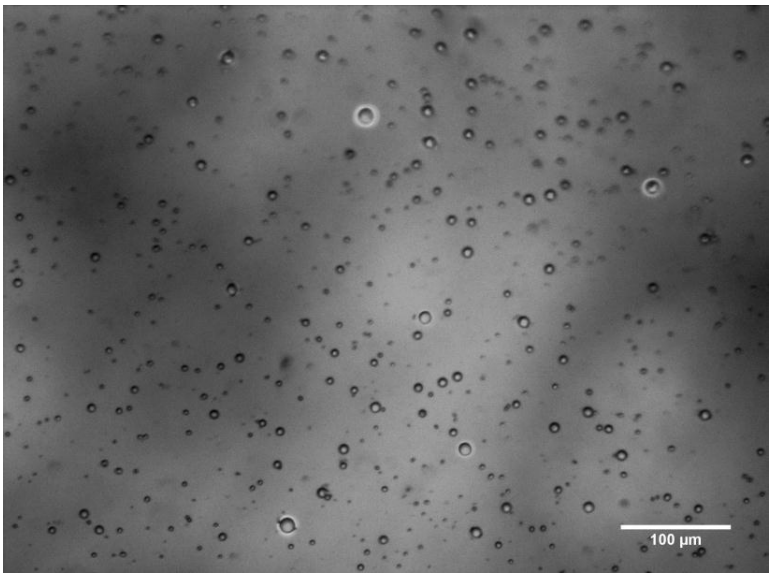

Figure 2.3 Optical image of gelatin microbeads in oily phase prepared from 75 µg/mL gelatin solution (ratio between water phase and oily phase: 1:5, stirring speed: 1000 rpm and emulsifying time: 10 minutes)

2.4.1.2 Effect of stirring speed on the characterization of gelatin microbeads

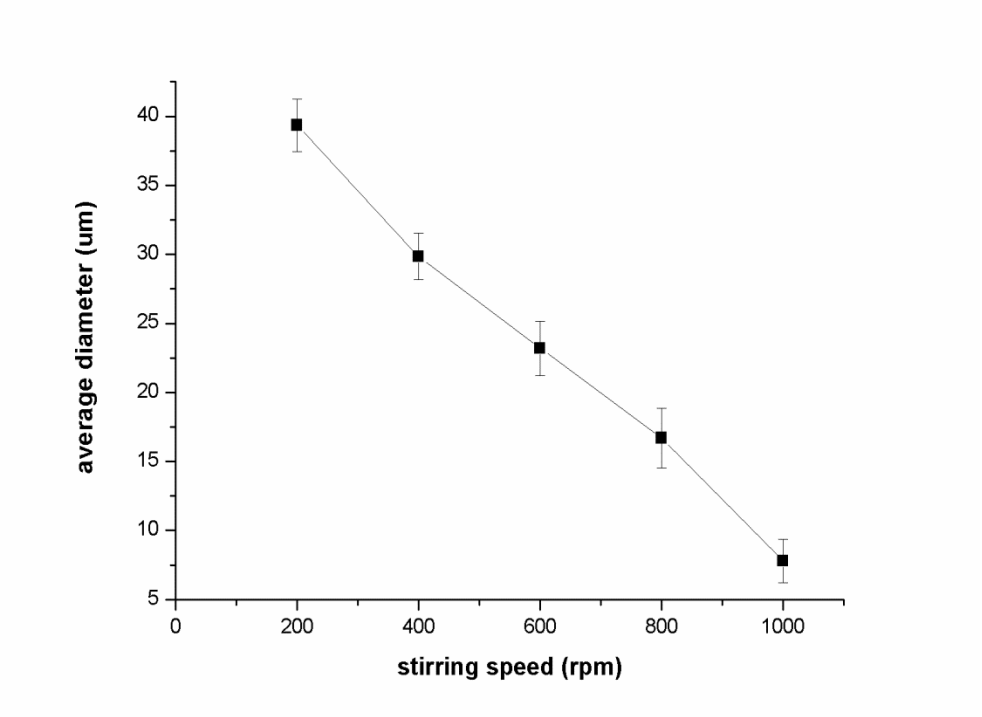

Figure 2.4 Average diameter of gelatin microbeads prepared at different gelatin concentrations (ratio between water phase and oily phase: 1:5, stirring speed: 800 rpm and emulsifying time: 10 minutes)

During the emulsification, five stirring speed of 200 rpm, 400 rpm, 600 rpm, 800 rpm and 1000 rpm were chosen to obtain different gelatin microbeads for comparison by fixing the ratio of 1: 5 between gelatin solution and oily phase, the concentration of gelatin solution of 100 μg/mL (10%) and 10 min of emulsifying time.

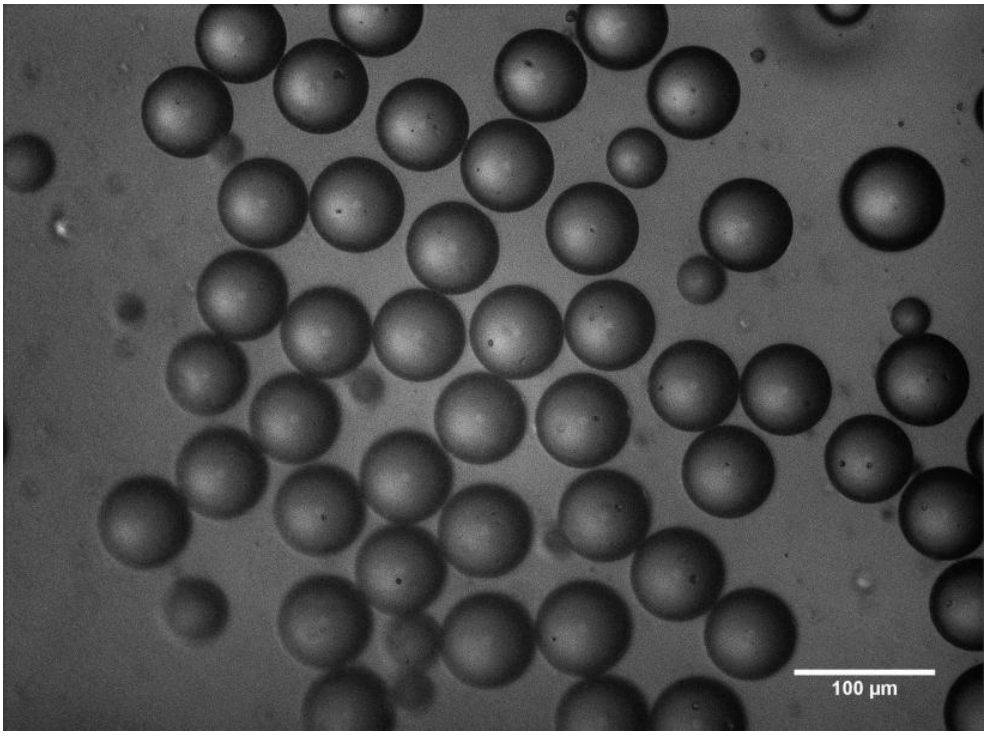

Figure 2.5 Optical image of gelatin microbeads in oily phase prepared from 150 µg/mL gelatin solution (ratio between water phase and oily phase: 1:5, stirring speed: 400 rpm and emulsifying time: 10 minutes)

As shown in Figure 2.4, particle size of gelatin microbeads resulted inversely proportional to stirring speed in the tested range. Water and oil phase were typically mixed in a 10 mL beaker with a 12 mm magnetic stirring bar. Under these conditions, low stirring speed of 200 rpm produced microbeads with a diameter of 39.3 ± 1.9 µm; nevertheless, high speed of 1000 rpm resulted in a much smaller diameter (7.8±1.6 µm). In addition, when the stirring speed is lower than 400 rpm, the distribution of the particle size is rather wide; there are a lot of small gelatin microbeads sticking to the big gelatin microbeads; while when the stirring speed is

higher than 1200 rpm, the phenomenon of agglomeration would become more and more serious. It could be explained that when agitation was carried out at lower speed, the water phase couldn't be dispersed into droplets efficiently with insufficient shearing force and the emulsion formed is not stable. Meanwhile, the gelatin microbeads tended to aggregate together to form the flocculation. Therefore, the size of microbeads obtained distributed in a wide range. However, with the gradual increase of stirring speed, the shearing force at each point of the emulsion increased progressively and became uniform, which led to the decreased diameter and narrower size distribution of gelatin microbeads. When the stirring rate continued increasing to a critical point, turbulence would form in the emulsion system, which brought uneven physical acting force on droplets. The occurrence of deformation and breakage due to the collision of droplets would increase dramatically, which resulted in the destruction of spherical-shaped microbeads and further inhomogeneity in size distribution[70, 90].

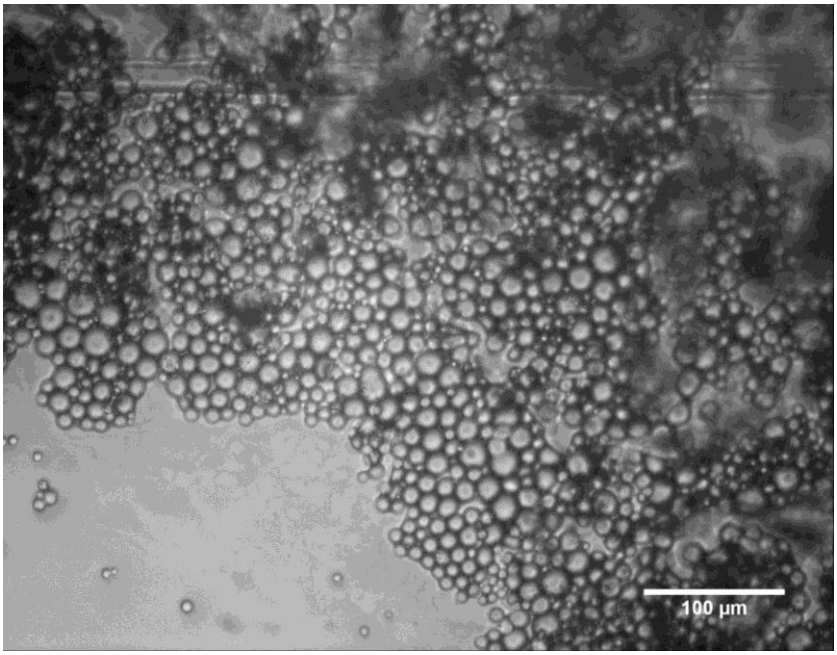

Figure 2.6 Optical image of gelatin microbeads in oily phase prepared from 100 µg/mL gelatin solution (ratio between water phase and oily phase: 1:5, stirring speed: 800 rpm and emulsifying time: 10 minutes)

Representative optical images of microbeads obtained under different conditions were presented. Large-sized microbeads (50.5 ± 16.4 µm) prepared at low speed of 400 rpm and from high-concentration gelatin solution of 150 µg/mL (15%) are shown in Figure 2.5; medium-sized microbeads (13.9±2.8 µm) prepared at medium speed of 800 rpm and medium concentration of 100 µg/mL (10%) are shown in Figure 2.6; small-sized microbeads (6.7 ± 1.8 µm) prepared at high speed of 1000 rpm and low concentration of 75 µg/mL (7.5%) are shown in Figure 2.3. Other conditions of all the images were the same: ratio between water phase and oily phase: 1:5 and emulsifying time of 10 minutes. The homogeneity of particle size declined with the increase of diameter.

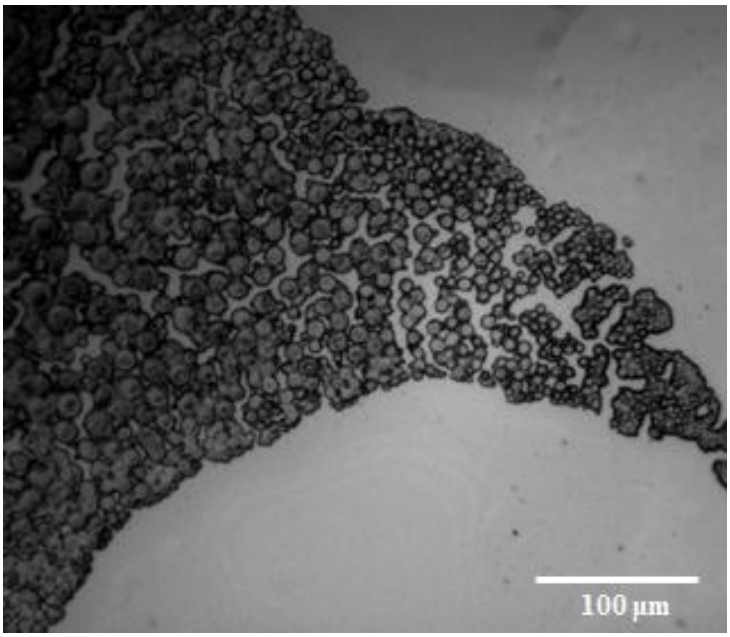

Figure 2.7 Optical image of treated gelatin microbeads prepared from 100 µg/mL gelatin solution (ratio between water phase and oily phase: 1:5, stirring speed: 800 rpm and emulsifying time: 10 minutes)

After several washings with n-hexane and then putting in a vacuum drier for one hour, the optical image of treated medium-sized gelatin microbeads was taken and presented in Figure 2.7. These microbeads are small, round and opaque.

After putting the treated gelatin microbeads into deionized water again, these gelatin microbeads started to absorb water and then became bigger and bigger, at last changed from opaque to transparent. The optical image was shown in Figure 2.8. They tended to stick to each other; however, it was very easy to make them uniform when under stirring. The big black dot

in the image was the residue of oil or n-hexane around the treated gelatin microbeads.

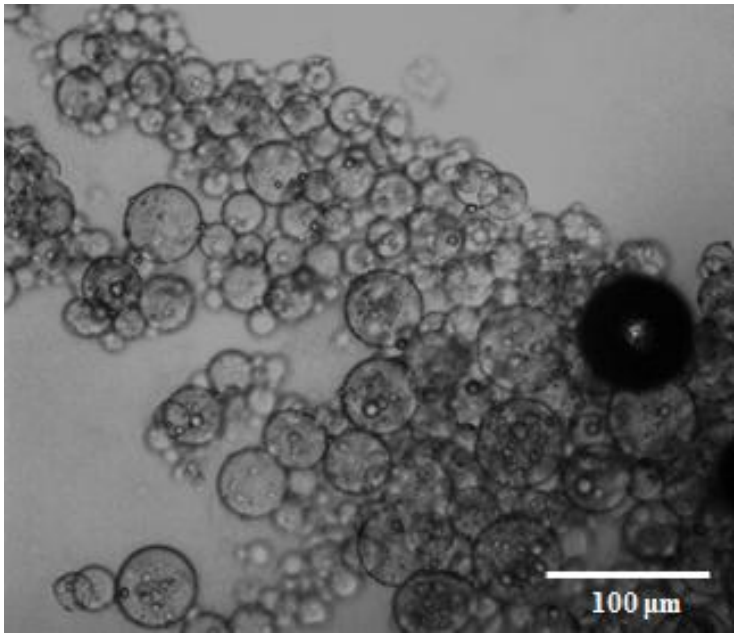

Figure 2.8 Optical image of treated gelatin microbeads after putting in deionized water prepared from 100 µg/mL gelatin solution (ratio between water phase and oily phase: 1:5, stirring speed: 800 rpm and emulsifying time: 10 minutes)

2.4.1.3 Effect of the ratio between gelatin solution and oily phase on the characterization of gelatin microbeads

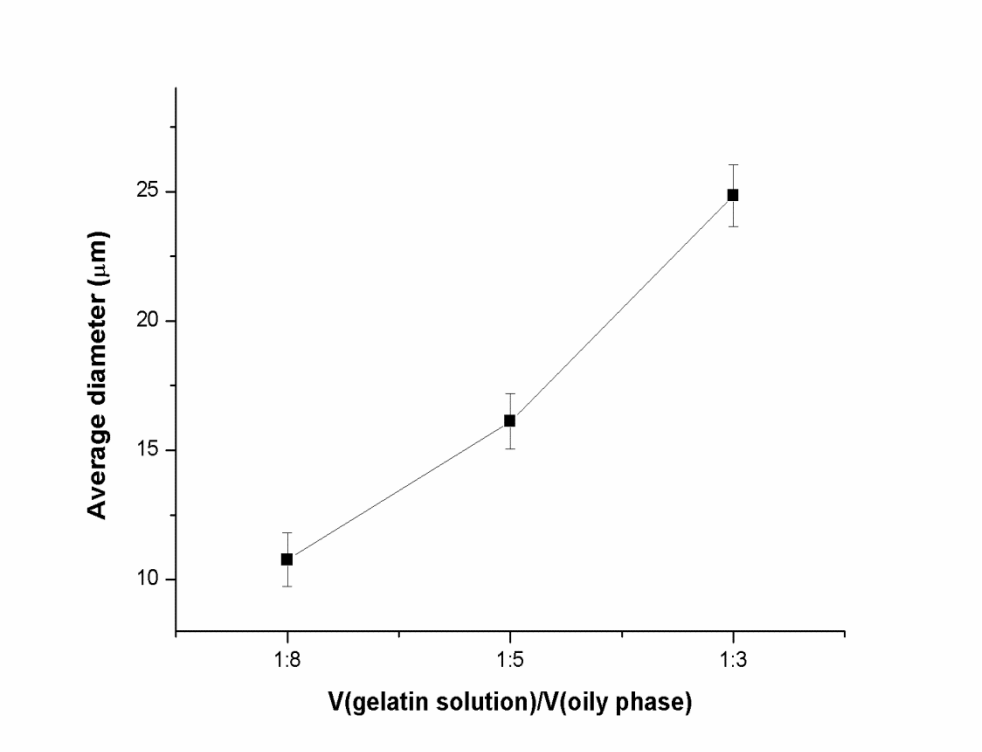

Figure 2.9 Average diameter of gelatin microbeads prepared at different ratio between gelatin solution and oily phase (concentration of gelatin solution: 100 μg/mL (10%), stirring speed: 800 rpm and emulsifying time: 10 minutes)

Besides the concentration of gelatin solution and stirring speed, another important parameter in the emulsion system is the ratio between water phase and oily phase, which had great influence on the morphology of gelatin microbeads.

The same as above, fixing other parameters, such as 100 μg/mL (10%) of the concentration of gelatin solution, 10 min of emulsifying time, 800 rpm of stirring speed, three different volume ratio between water phase and oily phase of 1:8, 1:5 and 1:3 were chosen to obtain different gelatin microbeads for comparison.

As shown in Figure 2.9, with the increase of water phase from 1:8 to 1:3, the particle size of gelatin microbeads increased from 10.9 ± 1.1 μm to 24.8 ± 1.4 μm. Based on the results, it could be concluded that decreasing the ratio between water phase and oily phase, the ability of oily phase to disperse the gelatin solution would be increased, which would lead to the formation of small gelatin microbeads.

2.4.1.4 Effect of emulsifying time on the characterization of gelatin microbeads

It takes some time for the dispersed phase to form the stable emulsion droplets under the external physical force. Therefore, to obtain the stable gelatin microbeads of good morphology and dispersity, the effective control of emulsifying time must be considered. Although emulsifying time had little influence on the particle size, it affected size dispersity and sphericity of gelatin microbeads, emulsifying time between 5 and 15 min made gelatin microbeads more homogenous and smoother. Emulsifying time less than 5 min or more than 15 min would result in the wide distribution of particle size and agglomeration of the gelatin microbeads, as shown in Figure 2.10 and Figure 2.11.

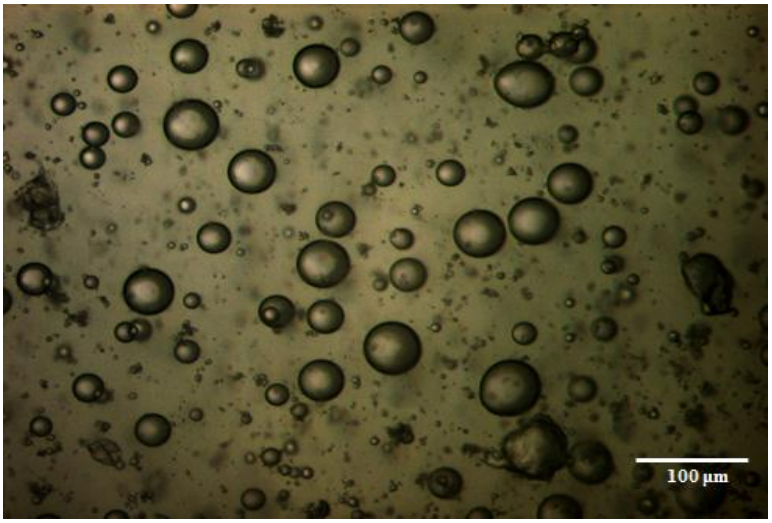

Figure 2.10 Optical image of gelatin microbeads in oily phase prepared under the following conditions: 100 µg/mL gelatin solution, volume ratio between water phase and oily phase: 1:5, stirring speed: 800 rpm and emulsifying time: 3 minutes.

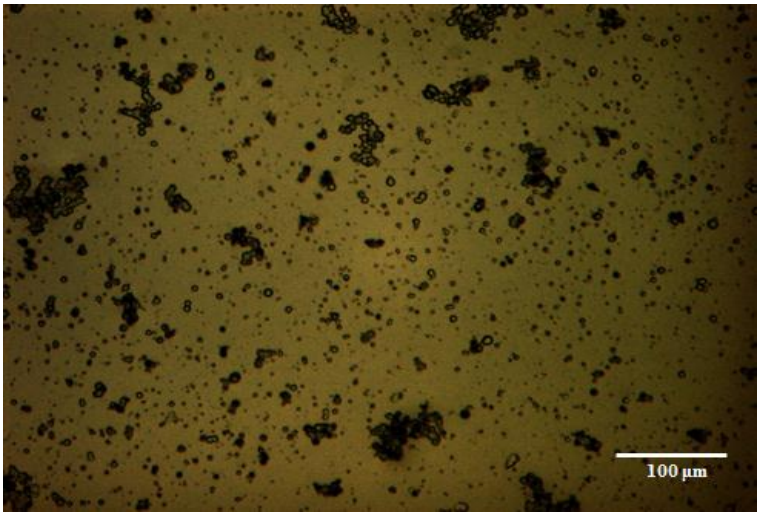

Figure 2.11 Optical image of gelatin microbeads in oily phase prepared under the following conditions: 75 µg/mL gelatin solution, volume ratio between water phase and oily phase: 1:5, stirring speed: 1000 rpm and emulsifying time: 18 minutes.

2.5 Conclusions

A series of gelatin microbeads were prepared through emulsification-coacervation method in water-in-oil (w/o) emulsion. The influence of preparation parameters on particle size, surface morphology and dispersity of gelatin microbeads was examined. The studied parameters include concentration of gelatin solutions, water phase/ oil phase ratio, emulsifying time and stirring speed. The experimental results indicated that increasing the concentration of gelatin solution would increase the particle size of gelatin microbeads linearly. The water/oil ratio had the same influence on the particle size as that of gelatin solution concentration. In addition, with the increase of water/oil ratio, the surface of microspheres became smoother as well. The emulsifying time had little effect on the mean diameter of gelatin microbeads, but it affected the dispersity of particles apparently. When emulsifying time was shorter than 5 min or longer than 15 min, gelatin microbeads had bad dispersity. The stirring speed had the similar influence as that of emulsifying time. Slow stirring rate made large size distribution and bad sphericity; excessive stirring speed resulted in aggregation likewise. The smaller size distribution and better sphericity of gelatin microbeads were observed under the stirring speed between 500 rpm to 1200 rpm.

In conclusion, increasing the concentration of gelatin solution or w/o ratio would increase the particle sizes of gelatin microbeads, proper emulsifying time and stirring speed would result in the narrow size distribution and best sphericity of gelatin microbeads. The excellent result was obtained with the condition: 100 μg/mL (10%) gelatin solutions, 1: 5 of

water/oil volume ratio, 10 min of emulsifying time and 800 rpm of the stirring speed.

Chapter 3

Drug delivery system of gelatin microbeads embedded in alginate

3.1 Introduction

The development of injectable drug-delivery systems has gained extensive attention over the last decade [91]. These systems possess unique advantages when compared to traditional administration routes, including localized and tissue-specific delivery, programmable release patterns, efficient loading and delivery, reduction of undesired side effects and minimally invasive administration [92, 93].

Recently, there has been growing interest in injectable hydrogels which can undergo solution-to-gel (sol-gel) transition *in situ* after injection in response to chemical or physical stimuli [94, 95].

A wide range of synthetic and natural polymer-based materials have been proposed to form injectable hydrogels for drug delivery and cell encapsulation. Back to 1997, Jeong et al. synthesized a thermosensitive and biodegradable injectable hydrogel consisting of PEO and PLLA blocks as drug delivery systems [96]; since then, a variety of block copolymers of Poly(ethylene glycol) and degradable, biocompatible aliphatic polyesters with tailored degradation behavior and hydrophobicity were proposed as hydrogel-based drug carriers [97-99]. However, it is generally complicated to standardize the synthesis of these custom-made block copolymers; in addition, their synthesis methods often involve toxic solvents and reagents that are difficult and expensive to remove, instability of the functional groups and low coupling efficiency.

Naturally-derived polymers have been largely used as hydrogels for drug delivery due to inherent bio-compatibility, bio-resorbability, bio-adhesive properties, and the resemblance to natural extra cellular matrix. Hydrogel-forming biopolymers include collagen and cross-linked gelatin, chitosan, agarose, fibrin and alginate [34, 100-103].

Injectable drug-loaded matrices and controlled release technology offer numerous advantages over conventional dosages. Cross-linkable alginate hydrogels have been proposed for in vivo injection, but their large initial burst release of encapsulated drugs represents a limitation for the transition to the clinical phase. To reduce this effect, a newly designed, cost effective, ease to prepare and very versatile drug delivery system for the encapsulation, delivery and release of hydrophilic molecules was demonstrated by combining uncross-linked, drug-loaded gelatin microbeads with cross-linkable alginate solution to generate a composite drug delivering hydrogel

in this chapter, the schematic representations of process was shown in Figure 3.1.

Hydrophilic fluorescein (FL) was chosen because it is a widely used model drug agent comparable with many chemotherapeutic drugs [104]. The release profile of FL from composite hydrogels was studied and compared with release profiles from the single constituents. In the gelatin/alginate composite hydrogel, the synergistic interplay between the two components overcomes the limitations of both alginate and gelatin gels. Gelatin offers a great flexibility in terms of available formulations and variety of drugs that can be incorporated. As shown in the chapter, gelatin microbeads help suppressing burst release and greatly extend the time span for sustained release when compared to alginate gel. On the other side, cross-linkable alginate is a very stable and practical carrier for gelatin microbeads and prevents gelatin from being immediately disperse upon melting after insertion in vivo. This new gelatin/alginate composite hydrogel shows a potential for the sustained release of hydrophilic molecules and the design of more versatile alginate-based injectable drug delivery systems.

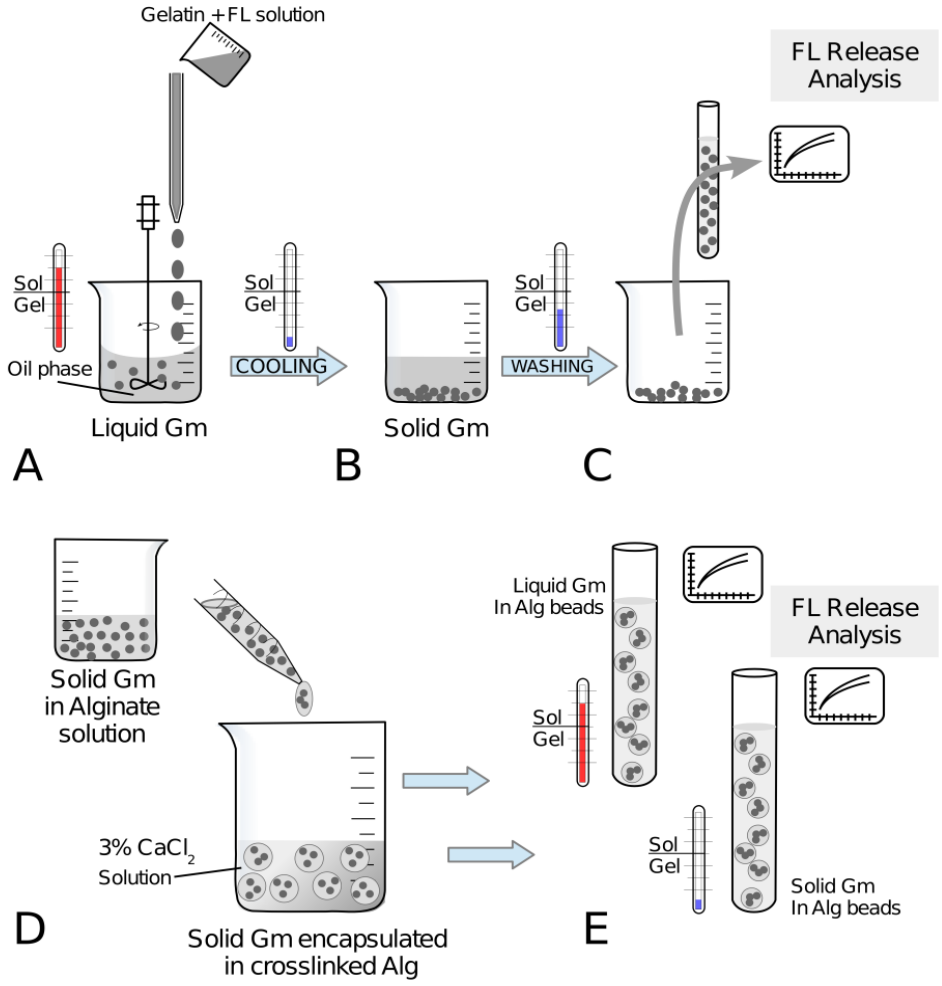

Figure 3.1 Schematic representations of the preparation of gelatin microbeads (Gm), encapsulation in cross-linkable alginate matrices and drug release analyses. A: preparation of liquid Gm loaded with FL by W/O emulsification in oil bath; B: cooling in ice-bath for complete gelation of Gm; C: extraction of solid Gm by hexane washing and release analysis; D: cross-linking of alginate gels encapsulated with solid Gm in $CaCl_2$ solution; E: drug release experiments from composite gels at RT (solid Gm) and 37 ℃ (liquid Gm).

3.2 Materials

Gelatin (gelatin type A, gel strength ~ 300 g Bloom, from porcine skin), Sodium Alginate (Alginic acid sodium salt from brown algae), Fluorescein (FL), Calcium Chloride, soybean oil, nonionic surfactant sorbitane monooleate (Span® 80) and n-Hexane were purchased from Sigma-Aldrich (Milan, Italy). All the materials were used as received without further purification.

3.3 Methods

3.3.1 Preparation of FL-loaded gelatin microbeads

FL-loaded gelatin microbeads were prepared with a similar process as described in section 2.3.3 under the optimal emulsification condition: 100 μg/mL (10%) gelatin solution, 1: 5 of water/oil volume ratio, 10 min of emulsifying time and 800 rpm of the stirring speed, where fluorescent molecules were mixed directly into the gelatin aqueous solution prior to the emulsification. Different gelatin solutions were prepared with FL concentrations equal to 5, 20 and 40 μg/mL.

3.3.2 Confocal images of FL-loaded gelatin microbeads

Confocal images of FL-loaded gelatin microbeads were taken with the laser confocal microscope (Nikon A1, Tokyo, Japan).

3.3.3 Preparation of FL-loaded gelatin and in vitro drug release from FL-loaded gelatin/gelatin microbeads

A gelatin aqueous solution at a concentration of 10% (w/v) was prepared by dissolving gelatin powder in deionized (DI) water at 40 ℃ for 30 min. Fluorescein (FL) was mixed into the solution to obtain a concentration of 20 μg/mL. 3 mL of the solution was filled into a 10-mm dialysis tubes (Regenerated cellulose dialysis membrane, MWCO 3500, Spectra/Por®, Spectrum Lab., CA, USA) and natural gelation was allowed at RT. Each dialysis tube was placed into a beaker with 60 mL of DI water under mild agitation to test the release of FL in time. The release experiment was performed both at room temperature (23 ± 1 ℃) and at body temperature (37 ± 1 ℃); three samples were tested for each experimental condition. For comparison, gelatin microbeads obtained from 10% (w/v) gelatin solution with 20 μg/mL of FL were also tested for the release in the same conditions. Every hour 1 mL of surnatant was extracted from each sample to determine the FL content, and replaced with fresh DI water. All the extracted samples were stored at 4 ℃ in dark until all the time points were collected.

3.3.4 Preparation of FL-loaded cross-linked alginate gels

A 1% (w/v) alginate aqueous solution was prepared by dissolving alginate powder in DI water at RT under mild agitation for 2 hours and then moved to an ice bath. Here, previously prepared FL-loaded gelatin

microbeads were uniformly dispersed into the alginate solution by continuous stirring for 5 min as shown in Figure 3.1(d). The stirring was completed in the ice bath to avoid too much FL releasing from gelatin microbeads. Volumetric ratio of 3 to 1 for alginate solution to gelatin solution was used to prepare the samples. After stirring, the alginate solution with dispersed gelatin microbeads was immediately injected dropwise into a 3% (w/v) $CaCl_2$ aqueous solution to induce alginate cross-linking and to form macroscopic alginate beads carrying FL-loaded gelatin microbeads.

Table 3.1 Tested samples

Sample code	**Description**
Gm	Gelatin microbeads
Gb	Gelatin directly loaded with fluorescein in bulk
Alg-1.25	Alginate macrobeads loaded with 1.25 μg/mL fluorescein
Alg-5	Alginate macrobeads loaded with 5 μg/mL fluorescein
Alg-10	Alginate macrobeads loaded with 10 μg/mL fluorescein
Alg(Gm-5)	Alginate macrobeads encapsuled with Gelatin microbeads containing 5 μg/mL fluorescein
Alg(Gm-20)	Alginate macrobeads encapsuled with Gelatin microbeads containing 20 μg/mL fluorescein
Alg(Gm-40)	Alginate macrobeads encapsuled with gelatin microbeads containing 40 μg/mL fluorescein

With this process, gelatin microbeads prepared from different FL concentrations (5, 20 and 40 μg/mL) were incorporated in alginate; the obtained composite gels are hereinafter named Alg(Gm-5), Alg(Gm-10), and Alg(Gm-20). For comparison, alginate macrobeads directly loaded with FL were also prepared. In this case, alginate was dissolved in aqueous solutions of FL at concentrations of 1.25, 5 and 10 μg/mL. FL-loaded alginate macrobeads with different content of FL were produced (hereinafter Alg-1.25, Alg-5 and Alg-10). These FL concentrations were specifically calculated to obtain the same absolute content of FL present in the previously described Alg(Gm-5), Alg(Gm-10), and Alg(Gm-20) samples. All the samples and compositions were summarized in Table 3.1.

3.3.5 In vitro drug release from FL-loaded cross-linked alginate gels

Release studies of FL-loaded gelatin/alginate composite gels were conducted by adding 2 mL of deionized water to a vial containing alginate macrobeads, as presented in Figure 3.1(e). 1 mL supernatant of each sample was collected at predetermined time intervals for fluorescence intensity test and the same amount of deionized water was added. The collected samples were stored at 4℃ in dark until all the time points were collected. Drug distribution in the composite hydrogels was monitored by confocal microscopy before and during the release experiment. After 7 days of release, Alg(Gm-5), Alg(Gm-10), and Alg(Gm-20) composite hydrogels were immersed in PBS at 37℃ for 24 hours to re-dissolve cross-linked alginate and free unreleased FL and gelatin. After centrifugation, supernatant was collected and analyzed to measure FL content.

3.3.6 Calibration curve of FL in DI water

The stock solution of FL was prepared by dissolving 50 mg of FL into 1000 mL of de-ionized water. Dilute the resulting solution into several different concentrations for the standard curve, then analyze with a Tecan Infinite 200 microplate reader (Tecan Group Ltd., Männedorf, Switzerland) (excitation wavelength: 494 nm, emission wavelength: 521 nm), using the de-ionized water as the blank sample. The calibration curve of FL is shown in Figure 3.2.

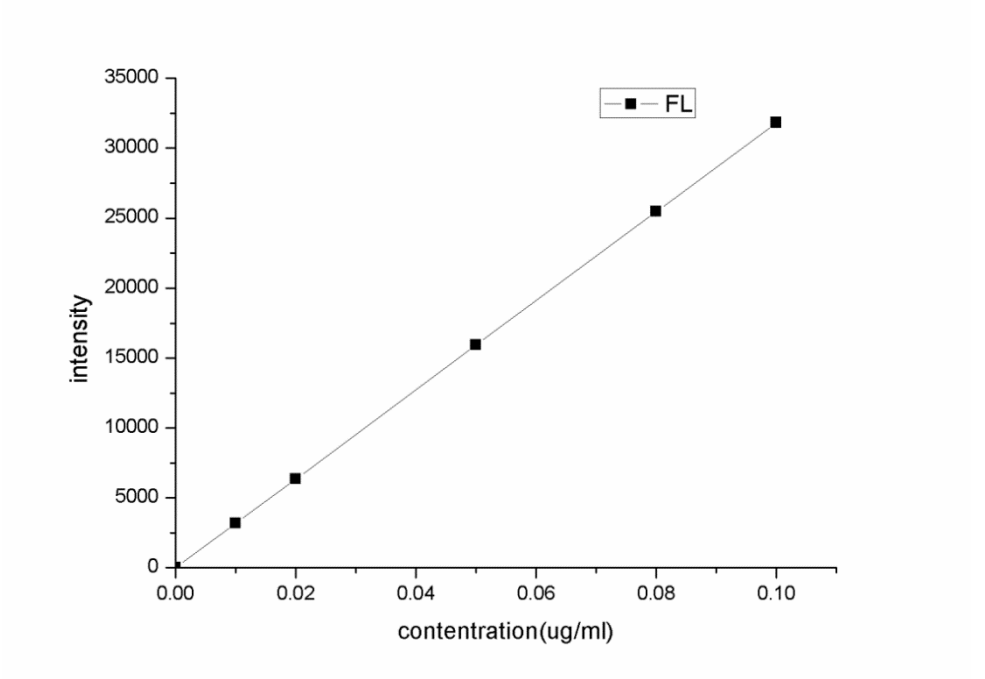

Figure 3.2 Standard curve of FL in DI water

The equation of the curve is: I=318263C with the correlation coefficient of 0.9999, where I and C denote the intensity of fluorescence and the concentration of FL, respectively.

3.3.7 FL release quantification and data analysis

Samples of 250 µL were placed in a 96-well microplate, and analyzed with a Tecan Infinite 200 microplate reader (Tecan Group Ltd., Männedorf, Switzerland) (excitation wavelength: 494 nm, emission wavelength: 521 nm) to quantify the concentration of released FL, according to the previously determined calibration curve. All measurements were performed in triplicates and release data were presented as mean ± standard deviation. Statistical analysis was performed using OriginPro software (OriginLab, Northampton, MA, USA) with significance level of $p < 0.05$.

3.4 Results and discussion

3.4.1 FL-loaded gelatin microbeads

The influence of gelatin concentration, stirring rate and emulsifying time on particle size, size distribution and dispersity was already investigated in section 2.4.2. We observed that microbeads with large diameter were characterized by larger size variability; while microbeads with smaller size had a strong tendency to agglomerate. Eventually, medium-sized gelatin microbeads (particle size 13.9 ± 2.8 µm) prepared from a 10% of gelatin solution at stirring rate of 800 rpm for 10 min were selected as drug carriers for the further examinations. The mid-size bead selection was consistent with previous papers demonstrating that microbeads smaller than 10 µm generally generate higher release rates due to the large mass transfer area [105, 106].

Representative confocal image of FL-loaded gelatin microbeads prepared under those conditions was presented in Figure 3.3. FL-loaded microbeads did not reveal significant differences in particle size and shape (homogeneous, spherical and narrow distribution) when compared to FL-free microbeads.

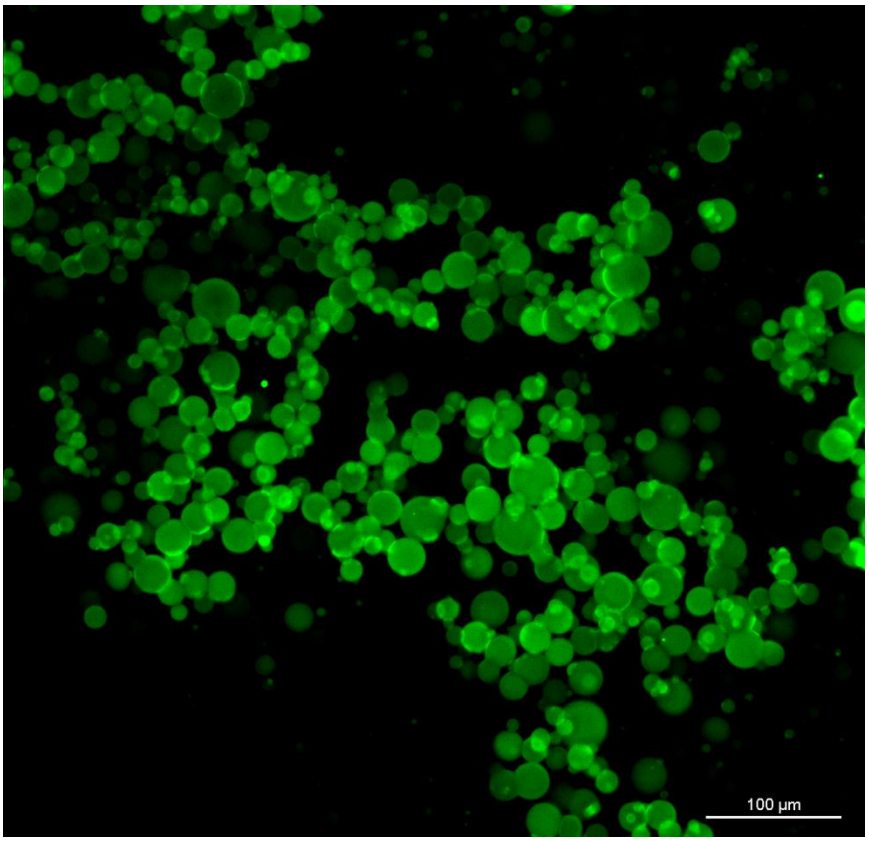

Figure 3.3 Confocal microscopy image of FL-loaded gelatin microbeads prepared from a 10% gelatin solution (stirring rate of 800 rpm and emulsifying time of 10 min)

3.4.2 In vitro FL release from gelatin gel and gelatin microbeads

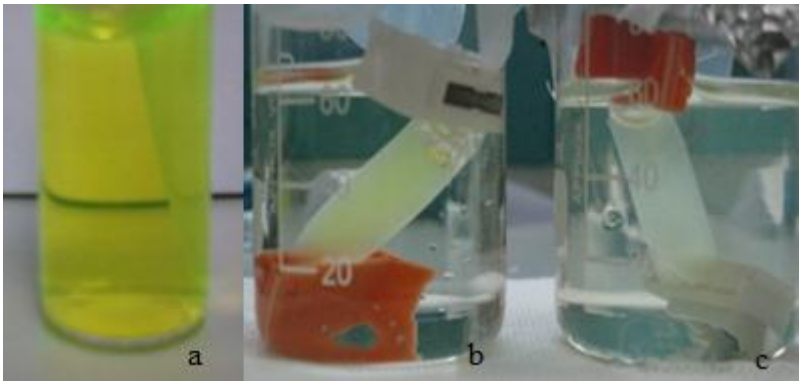

Figure 3.4 (a) FL-loaded gelatin gel, (b) after one-day release at RT, (c) after one-day release at 37 ℃

The images of FL-loaded gelatin gel before release test and after one-day release at RT and at 37 ℃ were presented in Figure 3.4. After one-day release, the colour of FL-loaded gelatin gel changed from yellow to light yellow. Moreover, after 6-hour release, the colour of FL-loaded gelatin gels at both temperatures almost stopped changing and the extent of colour change of the gel at 37 ℃ was deeper than the gel at RT, both of the phenomena were in accordance with the release profiles described as following.

The release profiles of FL from gelatin gel in bulk (Gb) and from gelatin microbeads (Gm) at both temperature were compared in Figure 3.5. The cumulative release of FL at 37 ℃ was significantly higher than at RT, both for Gb and Gm. At 37 ℃ gelatin microbeads showed a significantly higher initial burst release than gelatin gel in bulk, but, eventually, the cumulative

release value at the plateau reached a similar value for both materials (about 48%) after 10 hours. We noted that at 37 ℃, gelatin microbeads underwent a gel-to-solution (gel-sol) transition in a matter of minutes; while gelatin in bulk was completely dissolved in few hours. Cumulative releases at RT were 40% and 37% after 10 hours for gelatin microbeads and gelatin gel in bulk, respectively. In all cases, gelatin constructs had been separated by the surrounding medium by means of a dialysis membrane with a cut-off of 3500 Da to prevent the dispersion of the solubilized gelatin in the release medium after gel-sol transition.

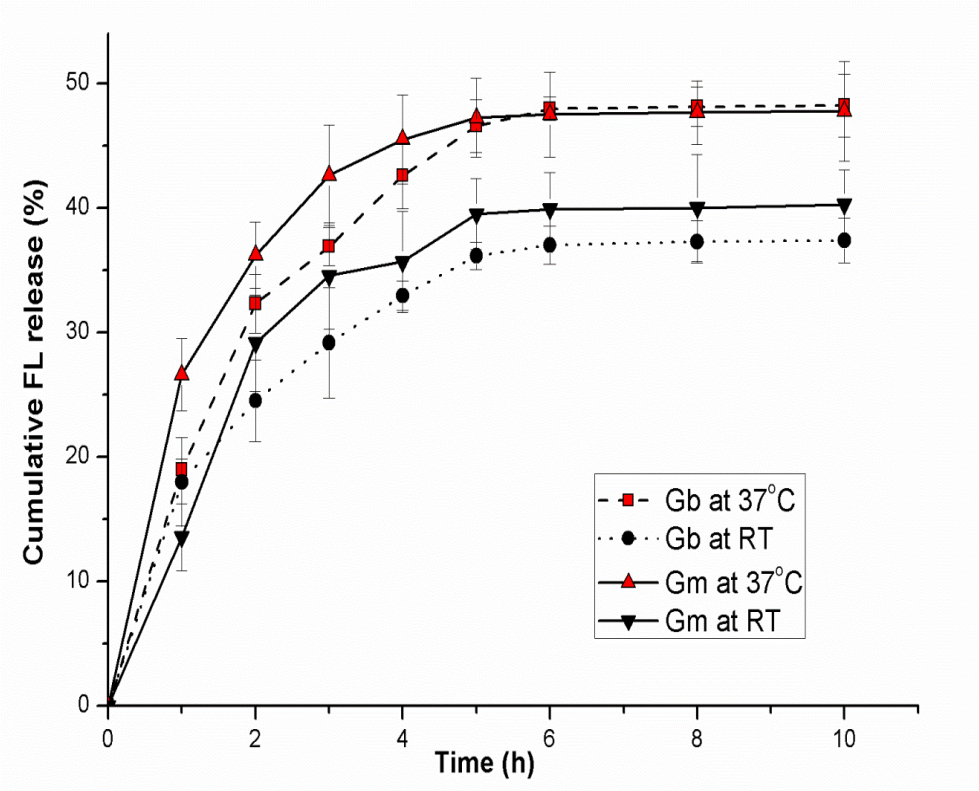

Figure 3.5 Release profiles of FL from Gb and from Gm at RT and at 37 ℃.

Even when the release profile reached the plateau, just about 50% of the loaded FL had been released in the surrounding medium; while more than 50% of the loaded FL remained bound to the gelatin proteins. The findings are in accordance with other works [35, 39]. Acidic FL and basic gelatin used in our study could form polyion complexation which limited the amount of the free drug and reduced the efficiency [32, 35]. In a previous study, Liao et al.[40] reported that a non-charged drug was completely released from alginate within 2 h, whereas charged drug compounds showed sustained release up to 3 weeks.

The possibility of an interaction between charged FL and gelatin is consistent with the high number of potential available basic sites in gelatin. Gelatin type A 300 Bloom has approximately an average molecular mass of 100 kDa, accounting for roughly 1100 total amino acids, and about 14% of the total amino acid residues are reported to have a basic character (positive charge) [26, 107]. On these bases, it is possible to estimate that the ratio between total number of basic gelatin sites and FL molecules can range from 1000 to 10000 depending on the FL concentration. However, as the number of really available basic sites depends on the acid-base equilibrium of the solution and can vary considerably with solution characteristics (pH and ionic strength), it is not possible to establish a univocal correlation between available sites and loaded FL molecules

It is clear that the extent of molecular interaction and chemical affinity between gelatin and loaded molecules depend on the physic-chemical characteristics of particular encapsulated molecule. As a consequence, a precise quantification of release efficiency and time span of sustained delivery of a specific active molecule has to be established case by case.

3.4.3 FL-loaded cross-linked alginate hydrogels with and without gelatin microbeads

(a) (b) (c)

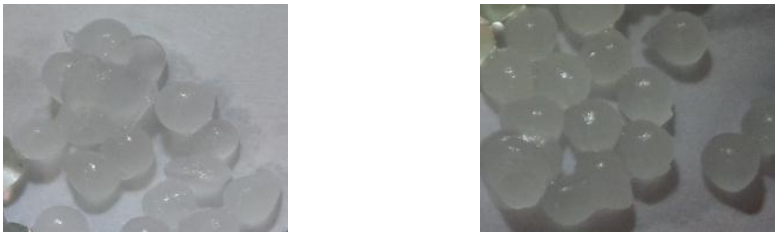

(d) (e)

Figure 3.6 (a) blank alginate droplets after cross-linking, (b) Alg-5, (c) Alg-10, (d) Alg(Gm-20), (e) Alg(Gm-40). Diameter of alginate droplets was about 3 mm.

Alginate was used as a carrier for gelatin microbeads. To model the release behavior of alginate in bulk, macroscopic spherical droplets of cross-linked alginate with a diameter of about 3 mm were prepared by adding dropwise alginate solution into a $CaCl_2$ solution. In Figure 3.6, it is possible to qualitatively appreciate the differences between naked cross-linked alginate droplets, alginate hydrogels directly loaded with FL, and alginate hydrogels carrying FL-loaded gelatin microbeads. Alginate gel appeared completely transparent and uncoloured (as shown in Figure 3.6 (a)). Alginate gel directly loaded with different concentrations of FL in

solution (Alg-5 and Alg-10) assumed a pale green color (Figure 3.6 (b) and (c)). Confocal image of the cross section of Alg-5 was presented in Figure 3.7; all the view was full of uniform green. Alginate gels encapsulated with FL-loaded gelatin microbeads (Alg(Gm-20) and Alg(Gm-40)) turned out to be opaque and whitish (Figure 3.6 (d) and (e)). As expected, by comparison between Alg-5 and Alg-10 or between Alg(Gm-20) and Alg(Gm-40), it was found that increasing FL content, the colour of alginate became more intensive.

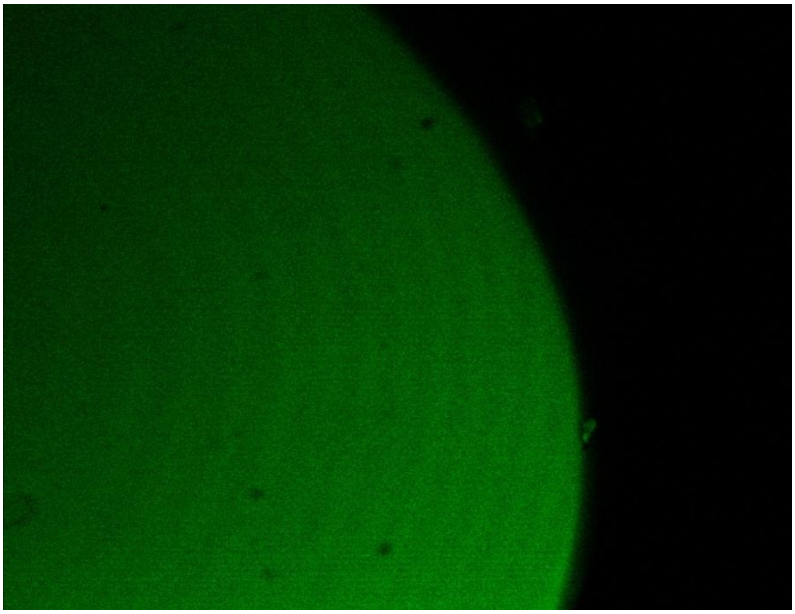

Figure 3.7 Confocal image of the cross section of Alg-5

At this stage, a brief stirring is necessary to uniformly disperse drug-loaded gelatin microbeads into the alginate solution. In this situation FL may diffuse from the gelatin microbeads into water-rich alginate solution. The extent of early release of FL into the alginate solution was estimated and accounted for 6% to 8% of the total FL content, depending on the mixing time (from 5 to 7 min). Most of FL was still trapped in the gelatin

microbeads, which was confirmed by the confocal micrograph as shown in Figure 3.8 (a).

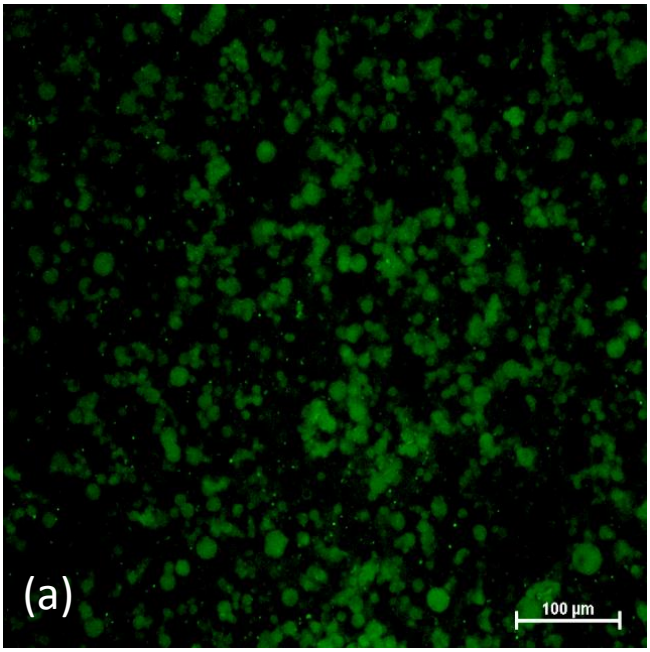

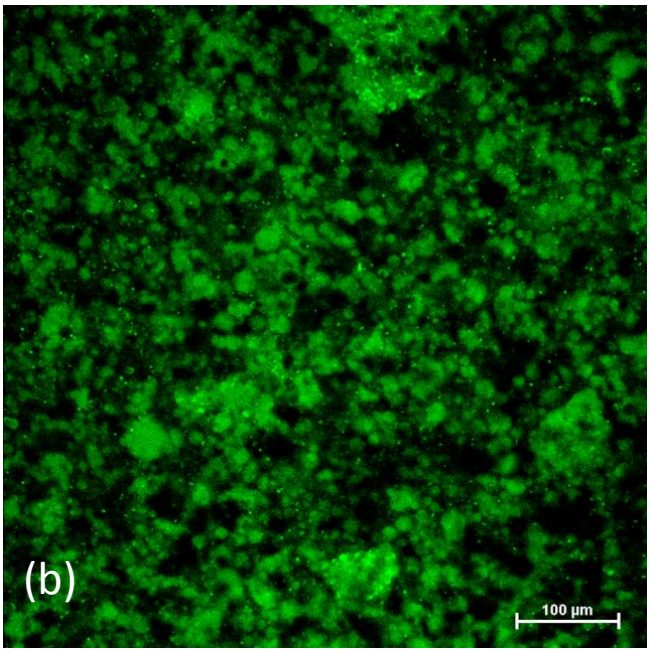

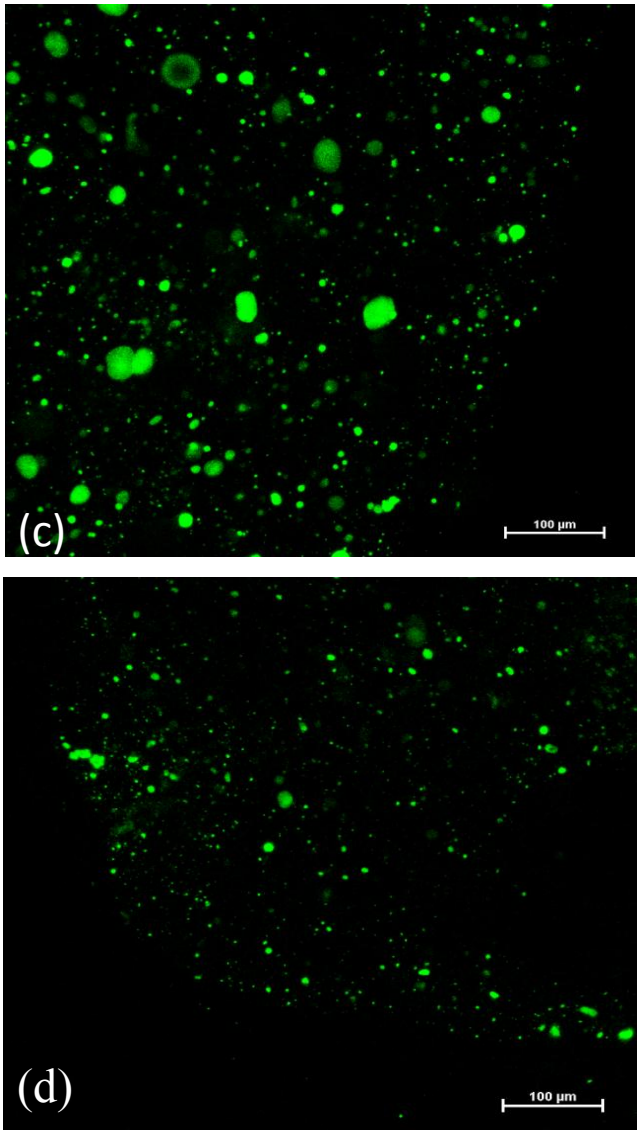

Figure 3.8 Confocal microscopy images of FL-loaded gelatin microbeads (Gm) encapsulated in alginate solution and cross-linked alginate gels: (a) Gm in liquid alginate solution before alginate cross-linking, (b) Gm in alginate hydrogel immediately after cross-linking, (c) Gm in alginate hydrogel after 24 hours of the release test at 37° C, (d) Gm in alginate hydrogel after 7 days of release at 37° C (scale bar =100 µm).

Drug loss from gelatin/alginate mixture to $CaCl_2$ solution during alginate cross-linking was equally inevitable, but accounted for less than 4% of the total loaded FL after 5-min of immersion. The washing stage in hexane did not involve any significant losses of loaded molecules, due to the limited solubility of FL in organic solvents.

3.4.4 In vitro drug release from FL-loaded cross-linked alginate gel

The distribution of FL in the alginate/gelatin composite hydrogels after cross-linking was monitored by confocal microscopy. Representative confocal micrographs of sectioned alginate gels after different time intervals were shown in Figure 3.8. In the first stage after mixing and alginate cross-linking, a fraction of free FL was readily released from the gelatin microbeads and delivered to the surrounding alginate gel (Figure 3.8 (b)). However, as shown in Figure 3.8 (c), after just 24 hours of release, free FL was completely cleared out from the alginate gel, whereas gelatin microbeads retained a considerable amount of FL. Even after 7 days of release (Figure 3.8 (d)), the signal of FL could be detected very clearly in gelatin microbeads; while no FL was found in the alginate matrix. These qualitative results are confirmed also by the release profiles.

The release curves for alginate gels encapsulated with FL-loaded microbeads Alg(Gm-20) and the counterpart alginate gel loaded with free FL (Alg-5) are presented in Figure 3.9. It is worth to recall that overall Alg(Gm-20) and (Alg-5) samples were loaded with the same concentration of FL, equal to 5 μg of FL for mL of gel.

It is possible to see that composite gel allowed to significantly reducing the initial burst release. After 2 hours at 37 ℃, Alg-5 presented an initial burst release of about 30% of the total loaded FL amount, while Alg(Gm-20) released less than 5% of the loeded FL in the same time span. A similar initial burst result was observed at RT.

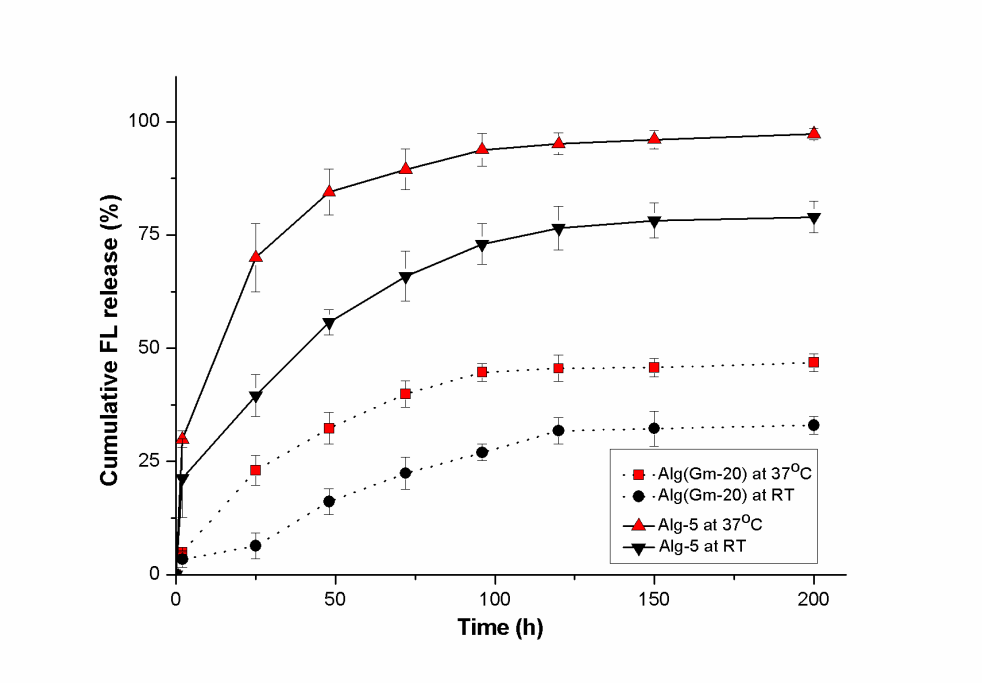

Figure 3.9 Release profiles of FL from FL-loaded gelatin microbeads encapsulated in cross-linked alginate (Alg(Gm-20)) and from cross-linked alginate directly loaded with FL in solution (Alg-5) both at 37 ℃ and at RT. The net amount of FL initially loaded in both Alg(Gm-20) and Alg-5 was the same.

The release rate of FL from the composite gel Alg(Gm-20) in the first 48 hours was significantly lower than the release rate from Alg-5 at either temperature. The release efficiency (cumulative release at the plateau) was

considerably lower in case of Alg(Gm-20), both at 37 ℃ and RT. At 37 ℃, the net release of FL from Alg-5 increased rapidly and about 70% of the loaded drug was released 24 h after the start of the release experiment, and more than 95% FL was released after 5 days. In case of Alg(Gm-20), the cumulative release was less than 25% after 24 hours release, and, even after one-week of release, less than 50% was delivered. The same tendencies were also observed at both temperature tested.

By comparing Figure 3.5 and Figure 3.9, it is possible to notice how the alginate matrix helped to extend the release time of FL from gelatin microbeads with a consequent marked reduction in the release kinetic. On the other hand, the total net cumulative release remained unchanged. At the same time, the addition of FL-delivering gelatin microbeads to the alginate drastically reduced the initial burst release found in case of alginate matrices loaded with free FL. According to our expectations, this reduction in burst release was specific to anionic drugs (or cationic drugs if gelatin type B is used); this does not apply to non-ionic drugs.

Additionally, since electrostatic attraction appears to be a dominant factor for lowering the initial burst, the ionic strength of the release medium could also affect the extent of drug/gelatin interaction. As a consequence, the high ionic strength of extracellular fluids in in vivo conditions could further reduce initial burst and release rate.

3.4.5 Effect of drug-loading concentration on the release profiles

Alginate gels with or without gelatin microbeads have been compared by investigating the effect of different drug-loading concentrations on their

release profiles. As shown in Figure 3.10(a), alginate gels loaded with free FL (Alg-1.25, Alg-5, Alg-10) released about 80% of the total FL in 24 hours, and the remaining FL was almost completely delivered after 150 hours. The cumulative release after 150 hours was higher than 95% for all the initial FL-loading concentrations.

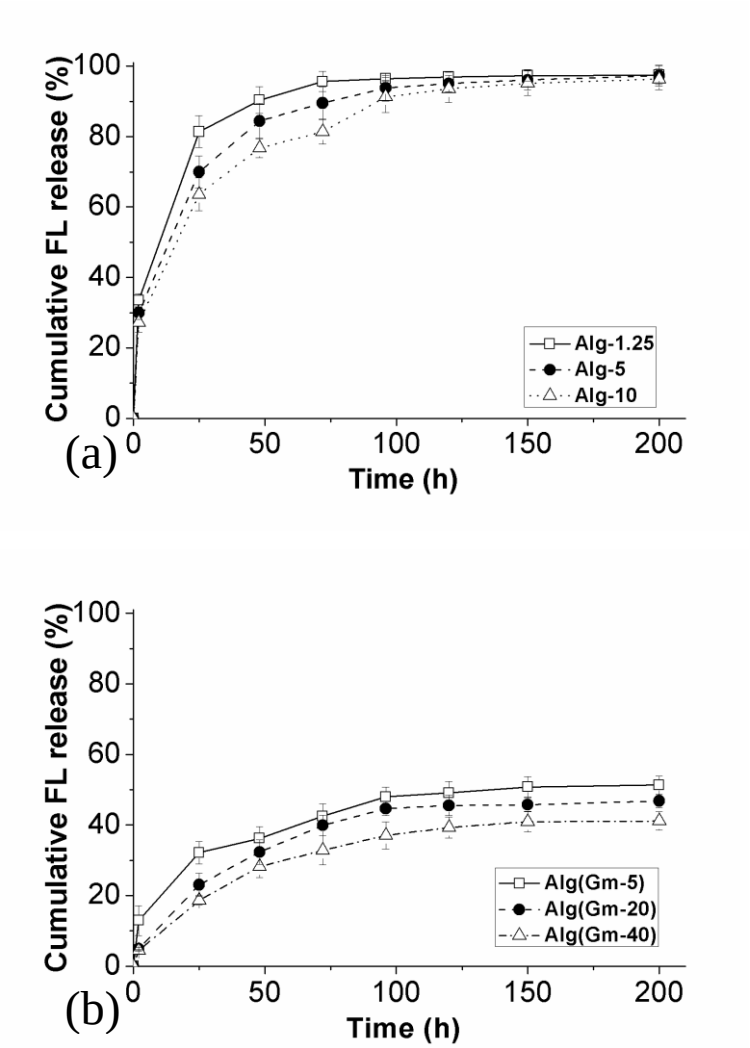

Figure 3.10 Effect of drug loading concentration on the release profiles of FL at 37 ℃: (a) from cross-linked alginate directly loaded with FL in

solution (Alg-1.25, Alg-5, and Alg-10), (b) from cross-linked alginate gels encapsulated with FL-loaded gelatin microbeads (Alg(Gm-5), Alg(Gm-20), and Alg(Gm-40)).

The release efficiency of FL from cross-linked alginate encapsulated with gelatin microbeads (Alg(Gm-5), Alg(Gm-20), Alg(Gm-40)) was significantly lower (Figure 10(b)), and in all cases the total cumulative release of gelatin-loaded alginate gels after 7 days was reduced to about 50%. On the other hand, initial burst release dropped from about 30% to less than 5% in the paired case of Alg-5 vs Alg(Gm-20) and Alg-10 vs Alg(Gm-40) and from 35% to about 15% in case of Alg-1.25 vs Alg(Gm-20). Sustained release was extended up to 200 hours. In general, comparing curves in Figure 10(b), it is possible to notice that higher loading concentrations resulted in lower drug release rate and efficiency; this fact is also in line with previous reports [39, 99].

Again, after the release process reached a steady state, just about 50% of the loaded FL had been released from the composite gels. This is consistent with the release profiles of FL from gelatin gels and microbeads presented in Figure 3.5. Confocal images in Figure 3.8(c) and (d) revealed that unreleased FL was still confined in the gelatin beads and probably bound to the gelatin proteins.

3.4.6 Versatility of composite gels and fate of the system in vivo

After 7 days of release, Alg(Gm-5), Alg(Gm-20), and Alg(Gm-40) samples were dissolved in PBS to free the remaining FL. As summarized in

Table 3.2, it was confirmed that more than 40% of the loaded FL was still trapped in the composite gels after the release. On the whole, more than 90% of the loaded FL was eventually detected. In addition, in this work a value of cumulative release at the plateau of about 50% of the loaded fluorescein was obtained. It is important to notice that this value is strictly dependent on the specific molecule that was used and the chemical affinity between gelatin and FL.

Table 3.2 Cumulative release after 7 days and delayed release after accelerated alginate dissolution in PBS from Alg(Gm-5), Alg(Gm-20), and Alg(Gm-40).

Sample	Cumulative release after 7 days (%)	FL detected after dissolution (%)	Total delivery (%)
Alg(Gm-5)	51.3 ± 2.5	42.6 ± 2.1	93.9 ± 3.3
Alg(Gm-20)	47.3 ± 2.3	44.2 ± 1.8	91.5 ± 2.9
Alg(Gm-40)	43.1 ± 2.6	46.7 ± 1.9	89.8 ± 3.2

In principle, release profiles and absolute value of cumulative release can be modulated independently, changing drug loading concentration in the gelatin microbeads, the alginate-to-gelatin ratio, and -- if possible -- temperature. This means that other molecules could have quite different release profiles and release efficiency before reaching the plateau. In some cases, almost complete release in a matter few hours was reported [41]. Ionically cross-linked alginate undergoes slow dissolution through ion exchange and is eventually absorbed by the body. As a consequence of alginate dissolution, gelatin and undelivered drugs are exposed to body

fluids. Uncross-linked gelatin then can be degraded by collagenase and other enzymes [108], and residual drugs bound to the gelatin can still be available for absorption.

In this study, we proposed to use a cross-linkable alginate solution as a carrier for drug-loaded gelatin microbeads. It has been previously reported that delayed cross-linking can be obtained with a number of different strategies [53, 60]. In some cases, alginate persists in a solution state long enough for the injection process to be completed; in other cases the forming alginate gel maintains a viscosity compatible with needle injection. In the present work, we used a fast gelation process to obtain consistently well-controlled alginate macroscopic spheres.

In fact, a well-controlled geometry was necessary to generate comparable and reproducible release data. However, considering that alginate gelation mechanisms are not influenced by the presence of gelatin, this drug-loading strategy could be applied to the previously demonstrated injectable alginate formulations.

3.5 Conclusions

A novel drug delivery system was demonstrated by encapsulating uncross-linked gelatin microbeads into a cross-linkable alginate matrix. The preparation of this composite hydrogel is extremely straightforward, fast and inexpensive; thanks to the mild operating conditions and the versatility of gelatin, virtually any hydrophilic drugs and molecules can be easily incorporated. The encapsulation of gelatin microbeads in the cross-linked alginate allowed a drastic reduction of initial burst release, while extending the sustained release of fluorescein up to 200 hours. Release profile can be easily modulated by varying drug-loading concentration in the gelatin microbeads, the alginate-to-gelatin ratio, and temperature. These results suggested that this alginate-gelatin composite hydrogel represented a potential improvement for self-cross-linking and injectable drug delivery system.

Chapter 4

Dual drug delivery system of gelatin microbeads embedded in alginate

4.1 Introduction

Since the first drug delivery system (DDS) was approved by FDA in 1989, DDS has been widely explored in the development of medicine and healthcare [73]. By using a DDS, especially sustained or slow drug delivery system, drug could be transported to the targeted site at predefined dose and time. Meanwhile, side-effect of tissue damage on extravasation, especially from high drug loading, could be reduced significantly. As a result of using DDS, problems such as poor solubility, poor biodistribution and rapid breakdown of the drug in vivo could be avoided effectively [5, 109]. However, because of diversification and complication of diseases and tissue reborn, the ability to deliver multiple drugs is often a pivotal factor to the efficacy of therapy.

For instance, after the orthopaedics and implant surgery, the therapies with multiple drugs are predominantly crucial to prevent bacterial infections, anti-inflammation, and improve osseo-integration or bone recovery [110-112]. Transporting multiple drugs in a system has been investigated increasingly and intensively. By employing various drugs at optimal dose and specific periods during the treatment, it would help DDS to reach the optimized effect and satisfy the needs in clinical therapies [113, 114]. Furthermore, different drugs for multiple-purpose therapy are also required in pharmaceutical and biomedical applications [66-69, 115]. In order to get optimal therapeutic effect of different drugs, the most important thing which should be considered is how to control release behaviour of each drug independently.

In this study, the composite of uncross-linked gelatin microbeads and cross-linked alginate was fabricated and used as dual drug delivery system, as shown in Figure 4.1. Based on our previous study[116], the synergistic interplay between the two components overcomes the limitations of individual component. Gelatin microbeads assist alginate to suppress the burst release and extend the duration of drug delivery; cross-linked alginate prevents gelatin microbeads from being immediately dissipated upon melting in vivo. In present study, two hydrophilic model drugs, Fluorescein (FL) and Rhodamine-B (RhB), were chosen to be encapsulated into alginate matrix and gelatin microbeads, respectively. These small fluorescent molecules are widely used as drug models for their ease to detect and are comparable with many chemotherapeutic drugs[104, 117].

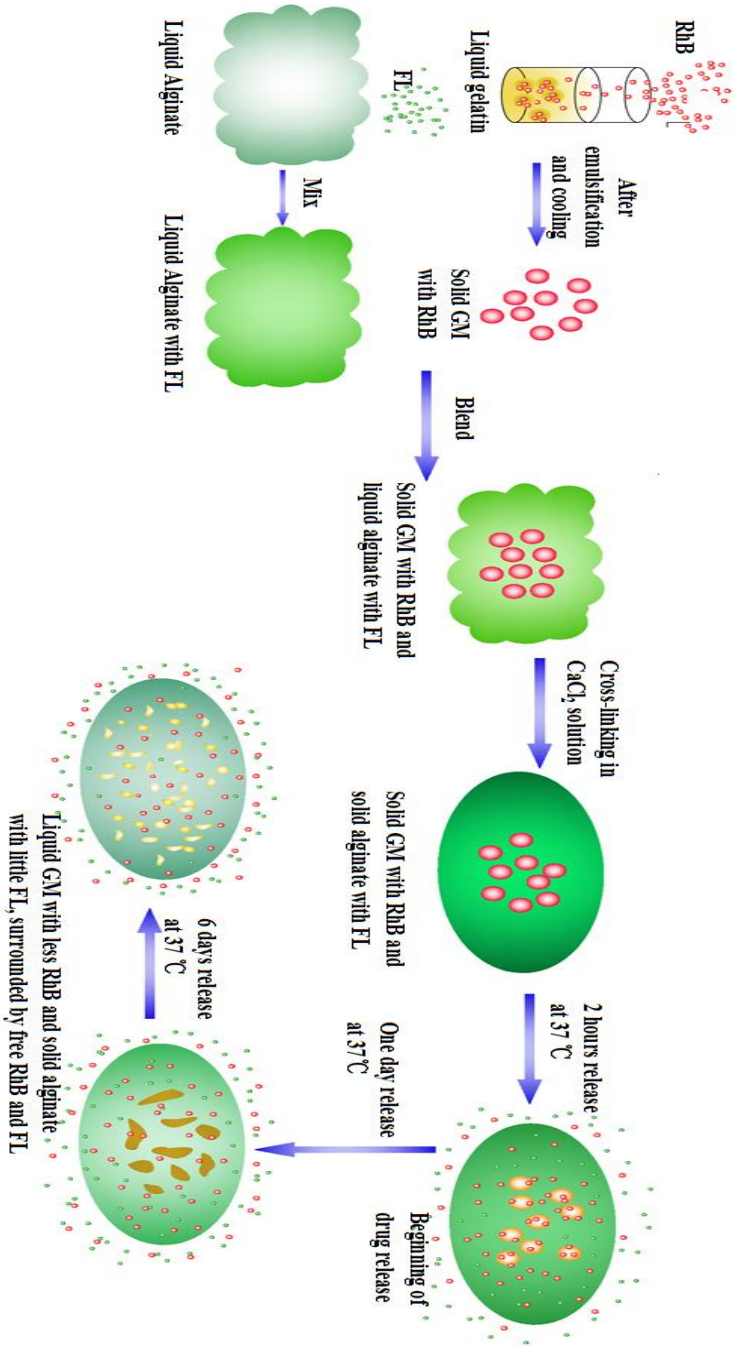

Figure 4.1. Schematic representation of the preparation of gelatin microbeads/alginate composite hydrogel and drug release.

RhB-loaded gelatin microbeads were first prepared and then dispersed in the aqueous solution of sodium alginate and FL. The resulting suspension was cross-linked upon the addition of calcium chloride solution to obtain the cross-linked composite hydrogel for dual drug delivery. The effects of drug-loading method of gelatin microbeads and the ratio between gelatin microbeads and alginate solution on the release profiles were studied. This composite hydrogel may show a broad application in multiple-drug delivery systems.

4.2 Materials

Gelatin (type A, from porcine skin), Sodium Alginate (Alginic acid sodium salt from brown algae), Fluorescein (FL) with green fluorescence, Rhodamine-B (RhB) with red fluorescence, Calcium Chloride, Trizma base, hydrochloric acid, soybean oil, nonionic surfactant sorbitane monooleate (Span 80) and n-Hexane were all purchased from Sigma-Aldrich (Milan, Italy). All the materials were used as received without further purification.

4.3 Methods

4.3.1 Preparation of RhB-loaded gelatin microbeads

A 10% (w/v) gelatin aqueous solution was prepared by dissolving gelatin powder (type A) in de-ionized water (DI water) at 40 ℃ for 30 min. RhB was mixed directly into the 10% (w/v) gelatin solution to obtain a 6 μg/mL RhB concentration.

Gelatin microbeads loaded with RhB were prepared by an emulsification method as described previously [116]. Briefly, 1 mL of RhB-loaded aqueous gelatin solution at the concentration of 10% (w/v) was added to 5 mL of soybean oil containing 100 mg of Span 80 while stirring at 800 rpm for 10 min in a 10-mL beaker with an 8-mm magnetic stir bar in a 40 ℃ water bath. The resulting water-in-oil emulsion was further stirred at 200 rpm for 30 min in an ice-bath for complete gelation of gelatin microbeads. The microbeads were washed five times with sufficient n-hexane and subsequently placed in a vacuum drier overnight to remove n-hexane. RhB-loaded microbeads produced with this process were identified as GM-1.

In addition, GM-1 microbeads were also frozen in liquid nitrogen and dehydrated by freeze-drying to obtain RhB loaded gelatin microbeads in dry state (hereinafter identified as GM-2).

In alternative, also RhB-free gelatin microbeads were produced starting from 10% gelatin solution without any dyes. In this case, RhB was loaded into the microbeads by immersing blank freeze-dried gelatin microbeads into a 6 μg/mL aqueous solution of RhB overnight (hereinafter identified as GM-3). All the samples were summarized in Table 1.

4.3.2 Morphology of gelatin microbeads

Confocal images of RhB-loaded gelatin microbeads in oily phase were taken with laser confocal microscope (Nikon A1, Tokyo, Japan). Surface morphology of gelatin microbeads was observed by scanning electron microscopy (SEM) (FESEM Field Emission Scanning Electron Microscope, ZEISS SUPRA™ 40, Göttingen, Germany). After freeze-drying, gelatin

microspheres were attached to the specimen stage with a double-side tape, and then spray-coated with gold at 0.6 kV before observation under the electron microscope.

4.3.3 Preparation of FL-loaded cross-linked alginate gels

Table 4.1 Samples prepared and their respective compositions

Sample code	Description
GM/GB	gelatin microbeads/ gelatin gel in bulk
GM-1	unfreeze-dried RhB-loaded GM
GM-2	freeze-dried RhB-loaded GM
GM-3	RhB-loaded GM by immerse free-loaded freeze-dried GM into RhB solution
Alg	FL-loaded alginate without GM
Alg(GM-1)	FL-loaded alginate encapsulated with unfreeze-dried RhB-loaded GM
Alg(GM-2)	FL-loaded alginate encapsulated with freeze-dried RhB-loaded GM
Alg(GM-3)	Immerse free-loaded freeze-dried GM into RhB solution, then mix with FL-loaded alginate and crosslink
2-Alg(GM-1)	FL-loaded alginate encapsulated with unfreeze-dried RhB-loaded GM, the same as GM-1, but with double alginate

A 1.5% (w/v) alginate aqueous solution was prepared by dissolving sodium alginate powder in DI water at RT under mild agitation for 2 h and then moved to an ice bath.

FL was first mixed directly in the 1.5% (w/v) alginate solution to obtain a FL concentration of 5 μg/mL. Then, previously prepared RhB-loaded gelatin microbeads (GM-1, GM-2 and GM-3) were uniformly dispersed into the FL/alginate solution by continuous stirring for 5 min in the ice bath. After stirring, 3% (w/v) $CaCl_2$ aqueous solution was immediately added on the top of the suspension. This made alginate cross-link and generated FL-loaded macroscopic alginate bulk carrying RhB-loaded gelatin microbeads. Composite gels carrying different GMs in this process are hereinafter named Alg(GM-1), Alg(GM-2), and Alg(GM-3). For comparison, FL-loaded alginate gels without gelatin microbeads named Alg and double volume of FL-loaded alginate gels carrying the same amount of GM-1 as in Alg(GM-1) named 2-Alg(GM-1) were also prepared. All the samples and compositions were summarized in Table 4.1.

4.3.4 Preparation of Tris-HCl buffer (pH=7.4)

To make a 1.0 M Tris buffer solution with pH equal to 7.4, 121.1g of Trizma base was added to 800 mL of DI water under mild agitation, after the temperature cooled down to RT, adjust the pH to 7.4 using 0.1 M hydrochloride. Finally, make the total volume of the buffer solution to 1 L by adding DI water. This solution could be stored at RT.

4.3.5 In vitro drug release from RhB-loaded gelatin gel and gelatin microbeads

To study the different drug release behaviors of RhB-loaded gelatin gel and gelatin microbeads, both of them were prepared from 1 mL gelatin aqueous solution containing 6 μg/mL RhB and then were filled into a 3 mm dialysis tubes (Regenerated cellulose dialysis membrane, MWCO 3500, Spectra/Por®, Spectrum Lab., CA, USA**)**. Each dialysis tube was immersed in 10 mL of Tris-HCl buffer solution (pH=7.4) under mild agitation. The release experiment was performed at 37 ± 1℃. At predetermined time intervals, 1 mL of release medium was extracted and replaced by 1 mL fresh medium. All the extracted samples were stored at 4℃ in dark until all the time points were collected.

4.3.6 In vitro drug release from FL-loaded cross-linked alginate gels

Different drug release studies from alginate gels with various components were conducted by adding 2 mL Tris-HCl buffer solution to a vial containing alginate gel. The release experiment was performed at 37 ± 1℃. 1 mL release medium of each sample was collected at predetermined time intervals for fluorescence intensity test and the same amount of Tris-HCl buffer solution was added. The collected samples were stored at 4℃ in dark until all the time points were collected. Drug distribution in the composite hydrogel (Alg(GM-1)) at different release stage was monitored during the release experiment by confocal microscope.

4.3.7 Calibration curve of FL and RhB in Tris-HCl buffer (pH=7.4)

FL and RhB were separately dissolved into Tris-HCl buffer solution at a concentration of 50 mg/L to prepare the stock solutions of FL and RhB. The resulting solution was diluted into several different concentrations for the standard curve, then analyzed with a Tecan Infinite 200 microplate reader (Tecan Group Ltd., Männedorf, Switzerland) (excitation wavelength: 494 nm, emission wavelength: 521 nm for FL; excitation wavelength: 560 nm, emission wavelength: 590 nm for RhB), using the Tris-HCl buffer solution as the blank sample. The calibration curves of FL and RhB are shown in Figure 4.2 and Figure 4.3.

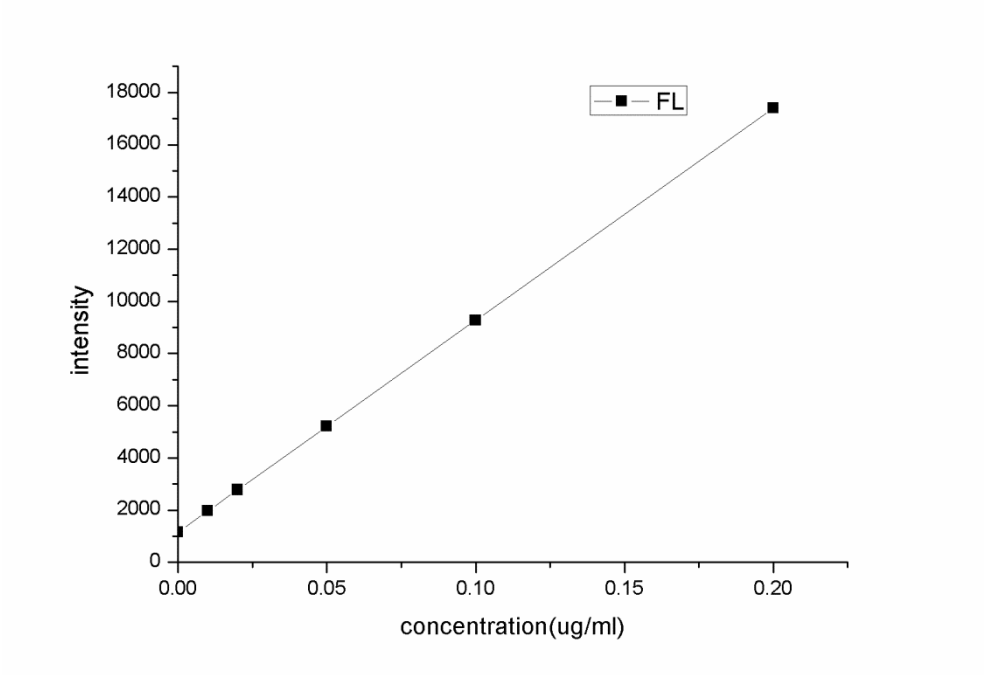

Figure 4.2 Standard curve of FL in Tris-HCl buffer solution

The equation of the curve is: I=81265C+1150 with the correlation coefficient of 0.9999, where I and C denote the intensity of fluorescence and the concentration of FL, respectively.

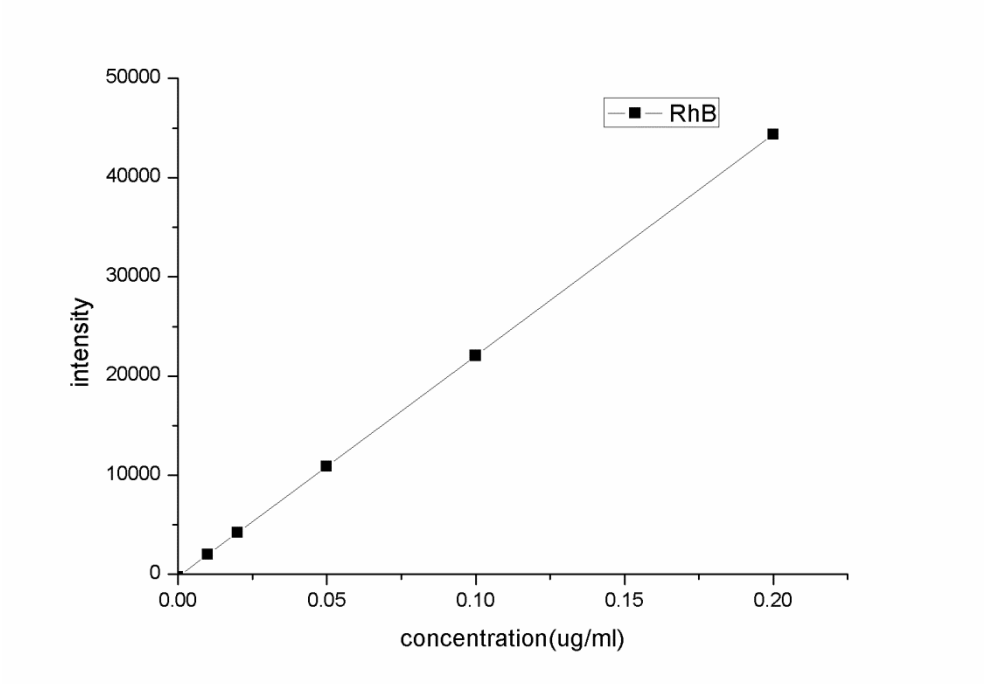

Figure 4.3 Standard curve of RhB in Tris-HCl buffer solution

The equation of the curve is: I=222852C-255 with the correlation coefficient of 0.9999, where I and C denote the intensity of fluorescence and the concentration of RhB, respectively.

4.3.8 Drug release quantification

Samples of 250 μL were placed in a 96-well microplate, and analyzed with a Tecan Infinite 200 microplate reader (Tecan Group Ltd., Männedorf,

Switzerland; excitation wavelength: 494 nm, emission wavelength: 521 nm for FL; excitation wavelength: 560 nm, emission wavelength: 590 nm for RhB) to quantify the concentration of released FL and RhB, according to the previously determined calibration curves, using the Tris-HCl buffer solution as the blank sample. All measurements were performed in triplicates.

4.3.9 Data analysis

All release experiments were carried out with at least three samples and all data were presented as mean ± standard deviation. Statistical analysis was performed using OriginPro software (OriginLab, Northampton, MA, USA) with significance level of $p < 0.05$.

4.4 Results and Discussion

4.4.1 Characterization of gelatin microbeads

It is well-known that morphology of the materials would be an appreciable factor in the drug release system [118]. The surface morphology of uncross-linked, freeze-dried gelatin microbeads was shown in Figure 4.4(a) and (b) in different magnifications. In Figure 4.4(a), an irregularly-shaped morphology of gelatine particles system was obtained due to the lack of crosslinking procedure. Lee [31] observed that the crosslinking process helps to shape the gelatin particles into a uniformly round morphology by the self-aggregation of gelatin particles. Those particles prepared in absence of crosslinking process display random morphology due to their inter-particle aggregation. Figure 4.4(b) presents the magnified morphology of

one single gelatin particle. Due to freeze-drying treatment, the losing of water made gelatin particle become porous, which we assume would led to fast drug diffusion from gelatin matrix according to Patel's study [119].

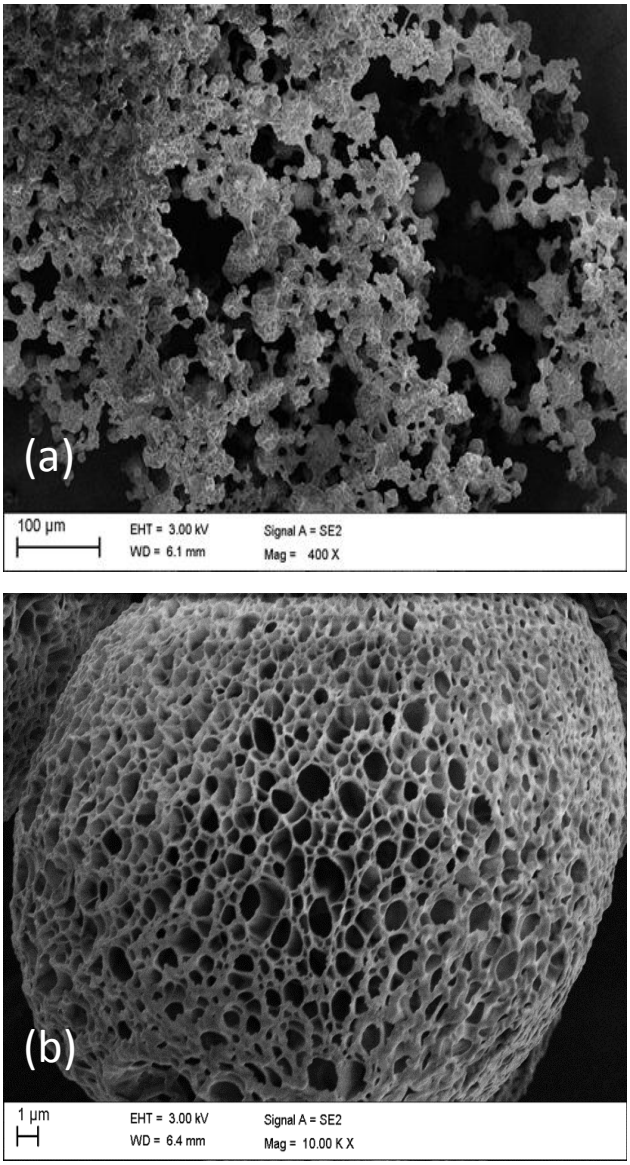

Figure 4.4 Scanning electron microscopic images of gelatin microbeads in low (a) and high magnification (b).

A representative confocal image of RhB-loaded gelatin microbeads in the oily phase was presented in Figure 4.5. From the figure we can see that the gelatin microbeads are spherical shaped in relatively uniform size distribution with an average diameter of 30 μm and the intensity of fluorescence is very strong.

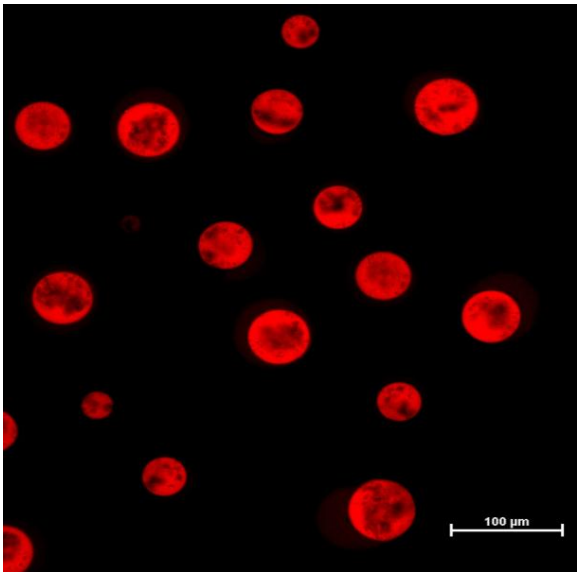

Figure 4.5 Confocal microscopy image of RhB-loaded gelatin microbeads (scale bar= 100 μm).

4.4.2 In vitro RhB release from gelatin gel and gelatin microbeads

The release profiles of RhB from gelatin gel in bulk (GB) and from gelatin microbeads (GM) at 37 ℃ were compared in Figure 4.6. RhB release from gelatin microbeads was slightly faster than that from bulk gelatin gel

during the first four hours, which was followed by a similar increasing tendency until a plateau (about 62%) was reached in both systems at 10 hours. We notice that at 37 ℃, bulk gelatin gel needs longer time than gelatin microbeads to undergo gel-sol transition, which can be assumed as the reason for the release difference in the first four hours. Then both of them reached the melt state under the same condition, that's why the two release curves almost overlap after four hours as shown in Figure 4.6. When release profile reached the plateau, the accumulative release percent of RhB was about 62%, which means about 38% of the loaded RhB still remained bound to the gelatin matrix for sustained and slow release. Similarly in our previous study, about 52% of the loaded FL was bonded to gelatin matrix [116], which suggests that the strength of the interaction deponds on the type of drugs used. According to Ofner's study [42], the duration of rapid release depends on the strength of interaction between gelatin and drug loaded. Gelatin contains a large amount of carboxyl, amide and amino groups, which would form different conjugates with different drugs. It is clear that the stability of the conjugates mainly depends on the molecular interaction and chemical affinity between gelatin and loaded drug. Moreover, prolonged drug impregnation increases the amount of drug complexed with gelatin [32]. In the case of our study, gelatin-RhB conjugate would reduce the amount of free drug to about 60%, therefore slow down the release rate of the rest drug, which is in accordance with other works [31, 32, 39, 40, 116].

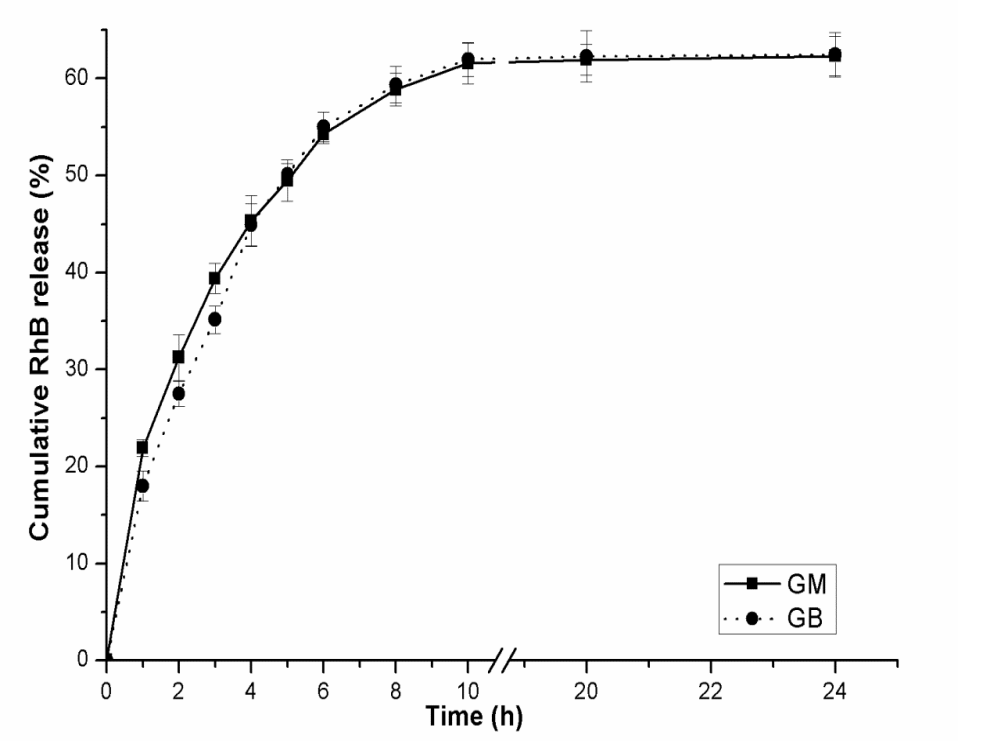

Figure 4.6 Release profiles of RhB directly from GM and GB at 37 ℃.

4.4.3 In vitro dual drug release from alginate/gelatin composite

At the stage of adding gelatin microbeads into alginate solution in an ice-bath, a fast stirring was necessary to uniformly disperse drug-loaded gelatin microbeads into alginate solution. Sample Alg(GM-1) containing different dyes (FL: green, in alginate; RhB: red, in gelatin microbeads) was observed at different period under confocal microscopy (Figure 4.7). Images in Figure 4.7A were taken before cross-linking. As shown in Figure 4.7(A-1), gelatin microbeads had a strong tendency to agglomerate [31]. The fluorescent

strength of FL in alginate solution where more gelatin microbeads contained was much stronger than where fewer gelatin microbeads existed because free FL tend to absorb on the surface of gelatin microbeads. This happens due to the fact that acidic FL could form stronger bonding with basic gelatin compared with the interaction between acidic FL and acidic alginate [41]. However, Figure 4.7(A-2) shows that fluorescence of RhB could be observed only in the gelatin microbeads instead of alginate solution, which indicates that the level of RhB released from gelatin microbeads to alginate solution was undetectable and RhB form stable bonding with gelatin. When fluorescence of FL and RhB were detected simultaneously as shown in Figure 4.7(A-3), the colour of gelatin microbeads turned from red shown in Figure 4.7(A-2) to yellow, which is one of the overlaid colour of red (RhB) and green (FL). This phenomenon further confirmed the absorption of FL by gelatin microbeads shown in Figure 4.7(A-1).

Drug loss from gelatin/alginate mixture to $CaCl_2$ solution during alginate cross-linking was inevitable, less than 3% of RhB and more than 20% of FL was detected, which were taken into consideration during calculation of their cumulative release.

Drug redistribution after two hours release in Tris-HCl buffer was presented in the images of Figure 4.7B. As shown in Figure 4.7(B-1), the background turned out to be lighter and more uniform in colour intensity, which suggests most of the FL was released. However, the concentration of FL in gelatin microbeads was still slightly higher than that in alginate gel, which indicates that FL could have stronger bonding with gelatin than with alginate [41, 42].

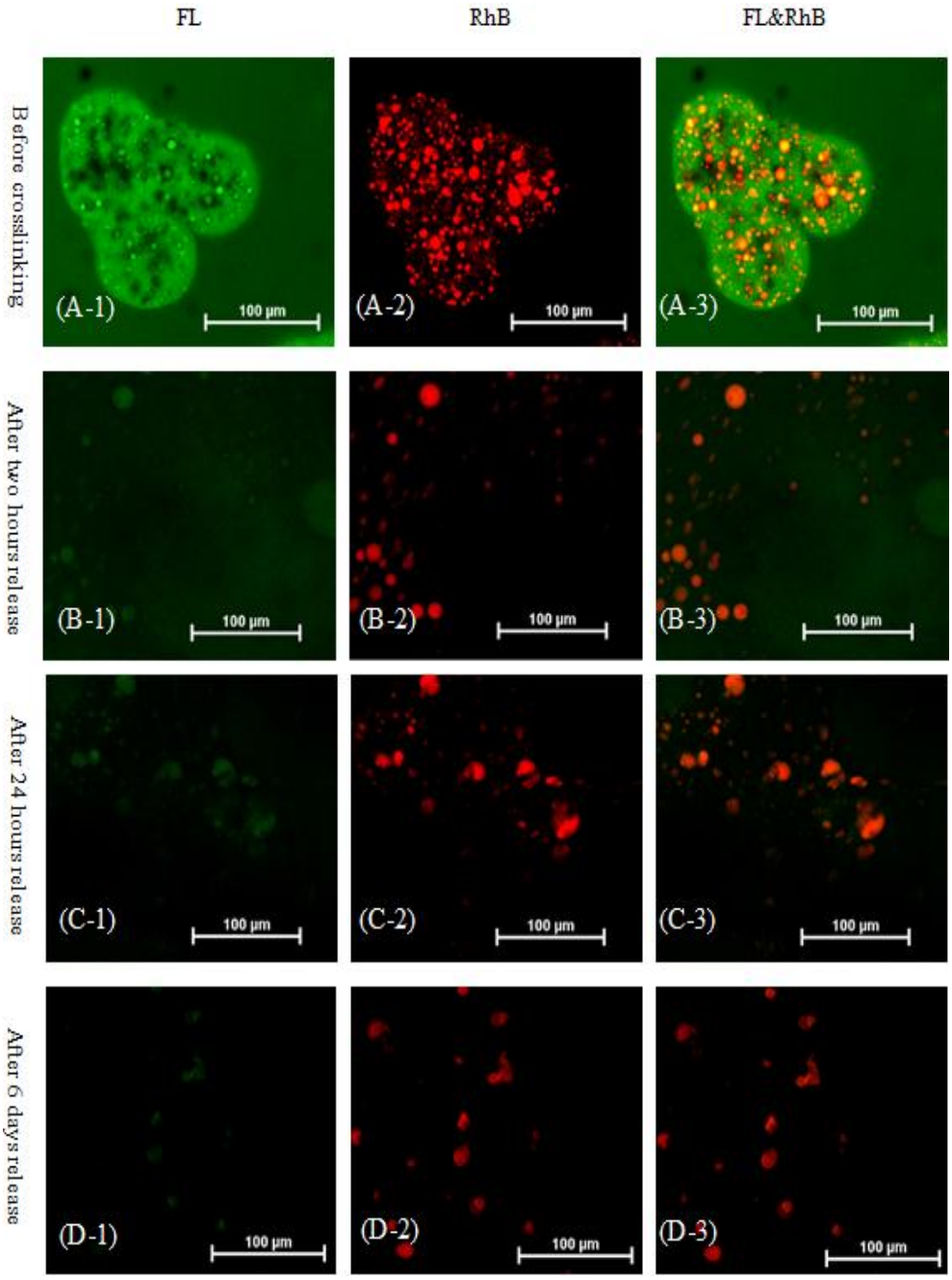

Figure 4.7 Confocal microscopy images of drug distribution at different release stage of composite hydrogel Alg(GM-1).

From Figure 4.7(B-2), we can see that most gelatin microbeads were still spherical but the colour of gelatin microbeads became lighter than those in Figure 4.7(A-2). We can assume that gel-sol transition of gelatin microbeads was still in process and the release of RhB just commenced. Due to the fact that both drugs can form more stable complex with gelatin than with alginate, after 24 hours release, the background of alginate gel became dark and weak green could be observed only in gelatin microbeads. Meanwhile, the shape of gelatin microbeads already turned to irregular, while the fluorescence of RhB in gelatin microbeads was still strong enough to monitor. Even after 6 days release (Figure 4.7(D-2)), the residual RhB could be apparently detected. However, by comparing Figure 4.7(D-2) with Figure 4.7(D-3), little difference could be recognized, which states that little FL was bonded to gelatin microbeads and was not capable of affecting the appearance of RhB. These qualitative results were confirmed also by the release profiles.

4.4.4 The comparison of two release profiles of FL and RhB

The release profiles of two drugs (FL and RhB) in sample Alg(GM-1) are shown in Figure 4.8. The two profiles have the similar release tendency but with quite different release percentage. With different bonding strength between drug and matrix, less than 40% of RhB was released after 24 hours; while more than 80% of FL was released out. From the comparison of confocal images shown in Figure 4.7, it was conformed that the 20% of residual FL was bonded to the gelatin microbeads instead of alginate matrix.

From 24 hours onwards, both FL and RhB were released slowly and continuously. Only 3% of FL and 7% of RhB were detected from the release buffer. However, with the dissolution of alginate matrix and the degradation of gelatin microbeads in the body, the release rate of the residual drugs would be fastened.

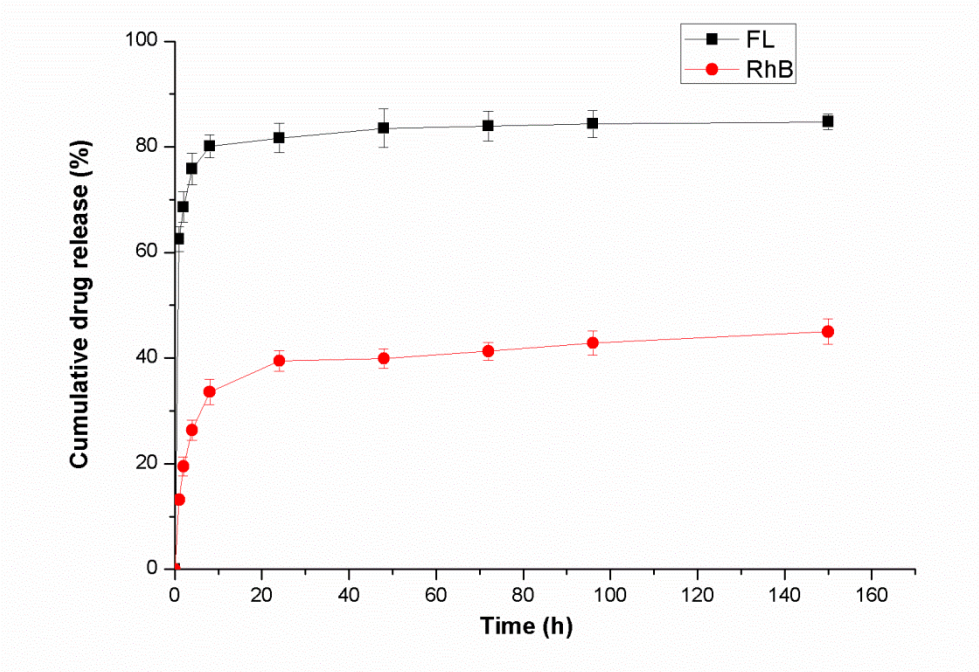

Figure 4.8 The comparison of two release profiles of FL and RhB from the sample Alg(GM-1).

4.4.5 Effect of loading ratio of gelatin microbeads on drug release profiles

The cumulative release curves of RhB from Alg(GM-1) and the counterpart with double amount of FL-loaded alginate gel 2-Alg(GM-1) are

presented in Figure 4.9, and the enlarged release profile during the first 8 hours is given in the inset of Figure 4.9. As reported [66, 118], drug loading amount would affect the drug release profile and high drug loading resulted in slower release, which is also proved in Figure 4.9. It could be seen that the tendency of both release profiles were similar, but the release rate of 2-Alg(GM-1) was faster than that of Alg(GM-1). This could be attributed to the change of drug diffusivity caused by the different drug loading levels and the varied microstructure in the composite. In addition, it was observed that more than 30% of loaded RhB was released in the first 8 hours, which estimated that not all the RhB molecules were ionically complexed with gelatin microbeads. It is probable that the non-complexed RhB was released by diffusion during the initial period of release [11, 16, 32, 65]. From day one onwards, the release was gradual and sustained. Approximately, 42% of the encapsulated RhB was released from Alg(GM-1) by day 6, which consistent with what was shown in confocal images.

By comparing with the release profile of GM in Figure 4.6, it is possible to notice that composite gel significantly reduced the RhB release rate and extended the release time. Only 10 hours was needed for alginate-free GM to reach the release plateau (62%). In comparison, less than 50% of loaded RhB was released from gelatin microbeads embedded with alginate matrix even after 6 days. As reported by Almeida et al, the change in the matrix structure would led to different release behaviour [120].

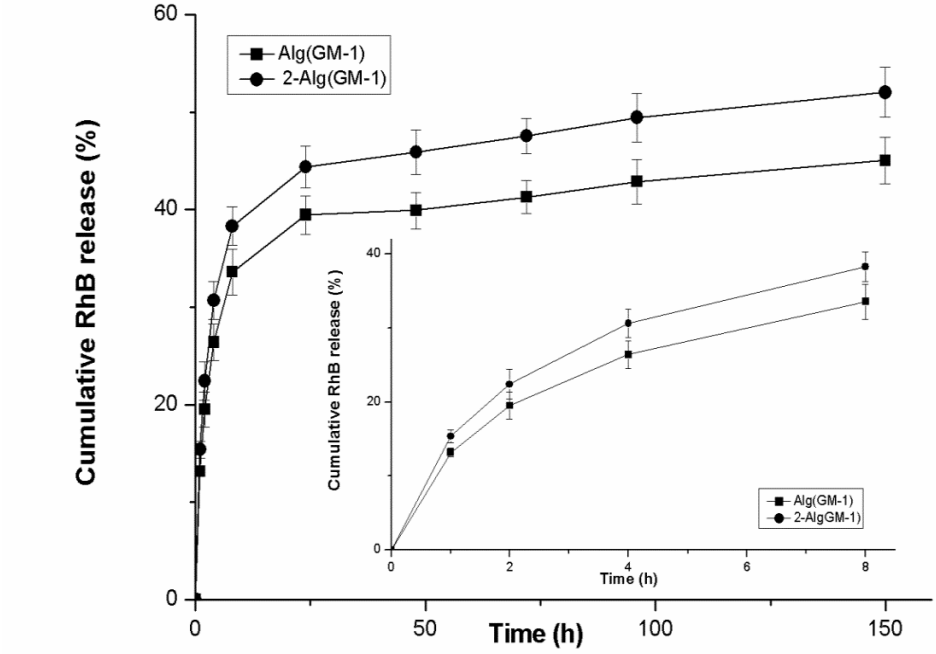

Figure 4.9 Effect of drug-loaded gelatin microbeads ratio on RhB release profiles of Alg(GM-1) and 2- Alg(GM-1).

It is reported that higher microbeads/matrix ratio resulted in faster drug release from matrix, which may be due to the interference introduced by microbeads to the matrix [66]. As shown in Figure 4.10, the release rate of microbeads-free alginate matrix (Alg) showed faster releasing rate than microbeads-loaded Alg(GM-1) and 2-Alg(GM-1), which was ascribed to the absence of gelatin microbeads. If there was no interaction between gelatin microbeads and FL, the FL release rate of Alg should be the lowest according to previous discussion. However FL forms bonding with gelatin microbeads, which slowed down the diffusion of FL from alginate matrix to

the buffer and then reduced the FL release rate of Alg(GM-1) and 2-Alg(GM-1). From the release curve of Alg(GM-1), it could be found that the release was fast in the first 2 hours with accumulative release of 70% FL. Cumulative release percent of FL till day 1 was approximately 85%, followed by a slow and sustained release till day 6, which could well illustrate the changes from Figure 4.7A to Figure 4.7D. The fast release before day 1 was mainly from the FL-alginate complex since the bonding between FL and alginate was weak. Nevertheless, the following slow release was from FL-gelatin complex, which was more stable.

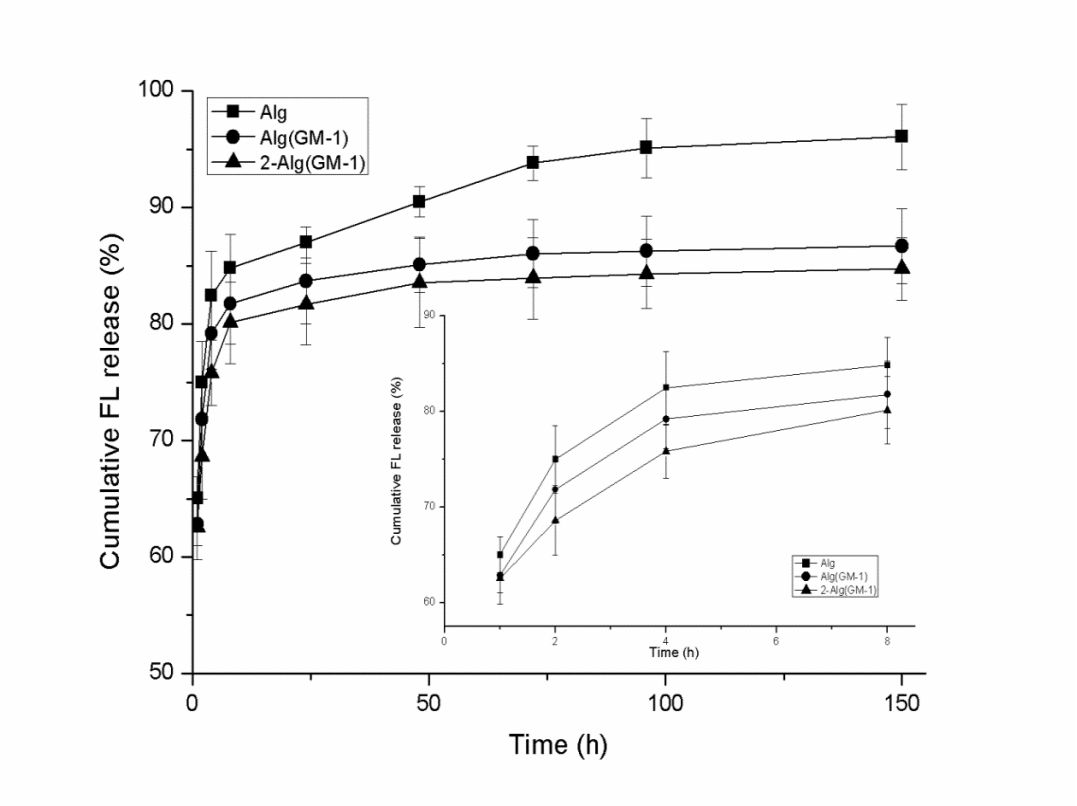

Figure 4.10 Effect of drug-loaded gelatin microbeads ratio on FL release profiles of Alg, Alg(GM-1) and 2- Alg(GM-1).

4.4.6 Effect of drug-loading methods of gelatin microbeads on drug release profiles

The effect of different preparation methods of drug-loaded gelatin microbeads on RhB and FL release profiles was studied. As shown in Figure 4.11, the cumulative release of RhB from Alg(GM-2) and Alg(GM-3) was much faster than that from Alg(GM-1). This could be explained by the fact that there was insufficient liberated water to dissolve freeze-dried gelatin micorbeads when encapsulated in the cross-linked alginate matrix. This resulted in rather weak bonding between RhB and freeze-dried gelatin microbeads in Alg(GM-2) and Alg(GM-3). Therefore, loaded RhB could cast off the bonding with gelatin easily and diffuse to the surrounding buffer. In addition, since the drug was loaded on Alg(GM-3) just by simple absorption, majority of the loaded RhB was concentrated on the surface of freeze-dried gelatin microbeads, which generated the fastest release among the three samples within first 24 hours.

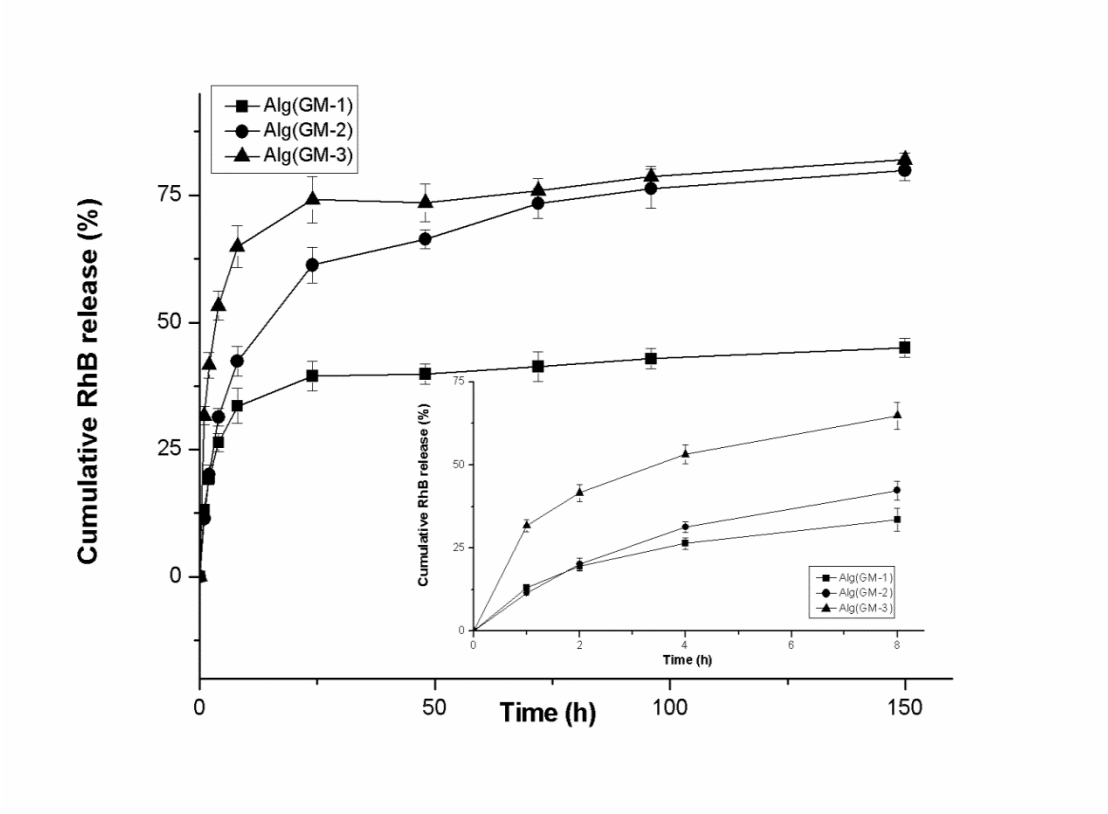

Figure 4.11 Effect of preparation method of drug-loaded gelatin microbeads on RhB release profiles of Alg(GM-1), Alg(GM-1) and Alg(GM-3).

FL release profiles from the three samples were demonstrated in Figure 4.12. Obviously, an initial quick release followed by a slow and sustained release was observed. As described above, release rate of RhB from Alg(GM-3) was the fastest, which implied the available sites for bonding FL increased. Therefore, just 75% of loaded FL was released even after 6 days compared with 80% of Alg(GM-2) and 85% of Alg(GM-1).

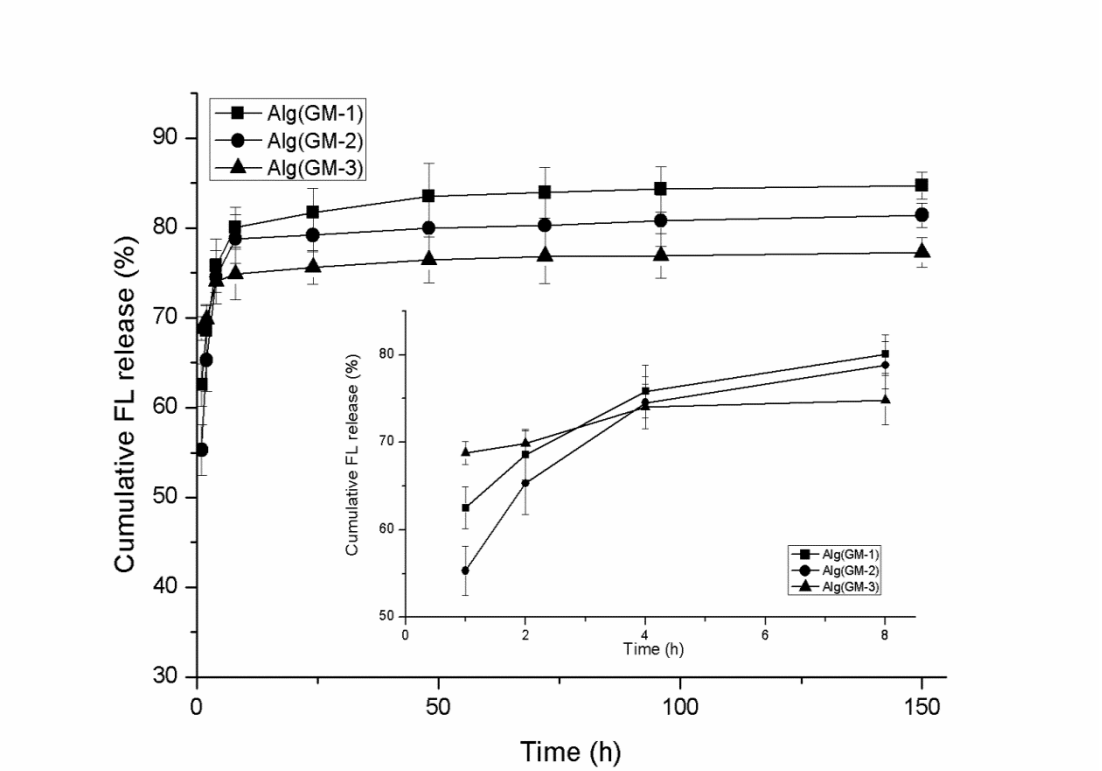

Figure 4.12 Effect of preparation method of drug-loaded gelatin microbeads on FL release profiles of Alg(GM-1), Alg(GM-1) and Alg(GM-3).

To summarize the releasing kinetics of independent drug in various systems, we can conclude that release rate of FL decreases in order: Alg>Alg(GM-1)> 2-Alg(GM-1)>Alg(GM-2)>Alg(GM-3) while RhB exhibits distinguished sequence: Alg(GM-3)>Alg(GM-2)>2-Alg(GM-1)>Alg(GM-1). Both FL and RhB present similar releasing tendency in Alg(GM-3). So from matrix point of view, it is reasonable to infer that Alg(GM-1) displays the most significant difference between the release of FL and RhB.

Although all the results in our experiment were based on the model drugs, this dual drug release technology seems to be applicable for many drugs or growth factors. Any charged molecules could be embedded in gelatin microbeads for sustained release since it is theoretically possible for gelatin to form polyion complexes with charged molecules, and another drug blended in alginate solution could be used for fast release. As for the practical application, after injecting or implanting the composite of gelatin and alginate into the body site, a slow dissolution of cross-linked alginate following the fast release would occur by removing the cross-linking ions in vivo, and then the remaining drugs bound with the gelatin microbeads would be released when gelatin microbeads lose the "protection" of alginate gel. Depending on the demand of practical application, adjusting the concentration of alginate gels would change the degradation time of alginate gels [49].

4.5 Conclusions

In this study, a dual-drug delivery system was fabricated by embedding gelatin microbeads within alginate matrices. The two components in the system helped to overcome the limitations of both alginate and gelatin gels in applications. The dual-drug release test in vitro showed quite different release profiles between FL loaded in alginate and RhB loaded in gelatin microbeads. The release profile of RhB illustrated a low initial release burst and cumulative release percent. Decreasing the ratio of RhB-loaded gelatin microbeads in alginate would increase the release of RhB and reduce the release of FL. In addition, RhB-loading method of gelatin microbeads had

significant influence on the release behaviour of both drugs. Moreover, gelatin microbeads after freeze-dry will shorten the difference between the release of FL and RhB. As a summary, the aim of this paper is to provide an idea for the field of dual drug delivery system, all the study is focused on the research in lab-scale which can be regarded as valuable reference for the practical application.

Chapter 5

Multi-drug delivery system of gelatin layers using agarose as diffusion barriers

5.1 Introduction

With the increase of the variety and complexity of diseases, multi-drug delivery system will be needed more and more in the future. Although loading individual drugs into conventional drug delivery systems has demonstrated to be a simple and efficient way, many disadvantages have come out, such as toxicity, poor bioavailability and bio-distribution [109, 121]. Supported by the results of chapter 3 and chapter 4, drug delivery systems based on gelatin turned to be a polymer-drug conjugates, where a drug would be covalently attached to gelatin to improve its therapeutic performance [122, 123].

The main improvement of multi-drug therapy over mono-drug therapy is the ability to delivery drugs to different disease as needed simultaneously, which results in increased activity and reduced toxicity [124, 125]. Moom et. al fabricated a multi-drug delivery system with sequential release based on the titania nanotube arrays in 2012 [126].

The aim of this chapter is to provide an idea for the multi-drug delivery system, although it is still immature for the application in vivo. Here, we prepared the multi-drug delivery system of gelatin layers by using agarose as the diffusion barriers, which is easy to prepare and doesn't need any organic solvent. Based on the performances of gelatin described in previous chapters, a series of gelatin layers loaded with different drugs were separated by the rods of agarose in a polycarbonate tube. With the change of the order of drug-loaded gelatin layers and the length of the rod of agarose, or temperature, different release profiles of multiple drugs could be obtained. However, for the device, it should be micro-sized, or at least millimeter-sized if using in the human body. In our experiment, we just preliminarily focused on the release effect with centimeter-sized device.

5.2 Materials

Gelatin (type A, from porcine skin), Agarose, Fluorescein (FL) with green fluorescence, Rhodamine-B (RhB) with red fluorescence, PBS buffer powder were all purchased from Sigma-Aldrich (Milan, Italy). All the materials were used as received without further purification.

5.3 Methods

5.3.1 Preparation of agarose solution and drug-loaded gelatin solution

A 2% (w/v) agarose aqueous solution was prepared by dissolving agarose powder in de-ionized water (DI water) at 95℃ for 30 min, then cooled down to 50℃ ready for use.

A 10% (w/v) gelatin aqueous solution was prepared by dissolving gelatin powder (type A) in de-ionized water (DI water) at 40℃ for 30 min. FL and RhB were mixed directly into the 10% (w/v) gelatin solution to obtain the concentration of 20 μg/mL of FL and 6 μg/mL of RhB, separately.

5.3.2 Preparation of the multi-drug delivery device and system

A hollow polycarbonate tube with sealed bottom was chosen as the drug delivery device. 200μL of RhB-loaded gelatin solution was injected into the bottom of the tube slowly. After the gelation of gelatin solution, a membrane of aluminum was put on the top of the gelified gelatin gel. There were several holes in the aluminum membrane.

The agarose solution was poured into the same type of polycarbonate tube. After the gelation, the gelified agarose gel was taken out and cut into pieces with different length, using as the diffusion barriers. A gelified agarose gel rod was put on the aluminum membrane.

Then another 200μL of FL-loaded gelatin solution and a gel rod of agarose were loaded into the tube one after another by the same method described as above.

To prevent the agarose gel going down after gelatin gel melted at body temperature, an aluminum membrane was put between each two layers. Finally, 2 mL of PBS buffer solution was added into the top of the second rod of agarose gel and then sealed with a film. The schematic diagram and the real picture of multi-drug delivery system were presented in Figure 5.1 and Figure 5.2.

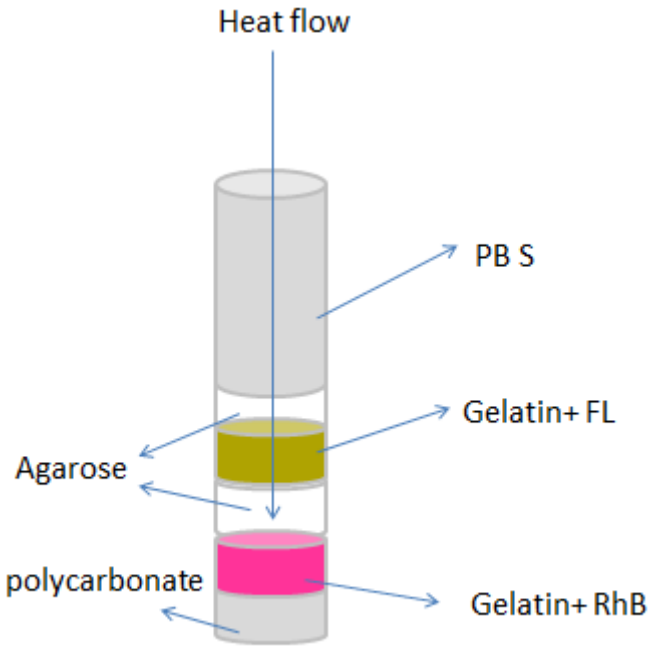

Figure 5.1 Schematic diagram of multi-drug delivery system.

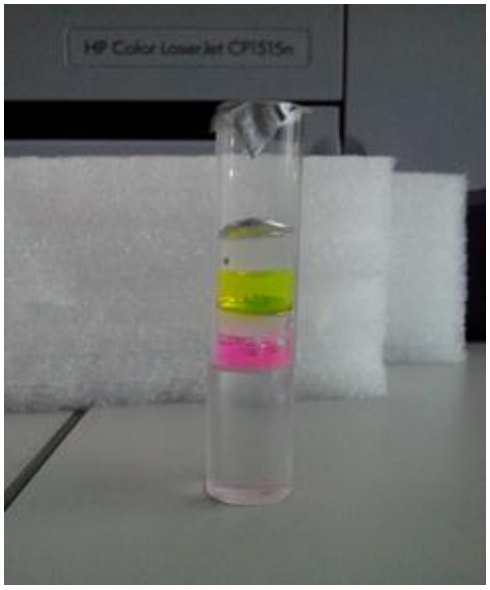

Figure 5.2 Picture of multi-drug delivery system

In this experiment, two factors were studied, temperature and the length of agarose gel; therefore, three different samples were prepared: two with 1 cm-length agarose gel, at different temperature (37 ℃ and RT); another one with 2 cm-length agarose gel at 37 ℃. All the samples and compositions were summarized in Table 5.1.

Table 5.1 Samples prepared and their respective compositions

Sample code	Description
L-FL	FL-loaded gelatin gel in the tube with 2 cm-length agarose gel at 37 ℃
L-RhB	RhB-loaded gelatin gel in the tube with 2 cm-length agarose gel at 37 ℃
S-FL	FL-loaded gelatin gel in the tube with 1 cm-length agarose gel at 37 ℃

S-RhB	RhB-loaded gelatin gel in the tube with 1 cm-length agarose gel at 37 ℃
S-FL-RT	FL-loaded gelatin gel in the tube with 1 cm-length agarose gel at RT
S-RhB-RT	RhB-loaded gelatin gel in the tube with 1 cm-length agarose gel at RT

5.3.3 In vitro drug release

The release tube was inserted into a cube of polyurethane to protect the temperature change inside of the release tube, and then put into different temperature environment. 1 mL release medium of each sample was collected at predetermined time intervals for fluorescence intensity test and the same amount of PBS buffer solution was added. The collected samples were stored at 4 ℃ in dark until all the time points were collected.

5.3.4 Calibration curve of FL and RhB in PBS buffer solution (pH=7.4)

The stock solutions of FL and RhB were prepared by dissolving 50 mg of FL and 50 mg of RhB into 1000 mL of PBS buffer solution, respectively. Dilute the resulting solution into several different concentrations for the standard curve, then analyze with a Tecan Infinite 200 microplate reader (Tecan Group Ltd., Männedorf, Switzerland) (excitation wavelength: 494 nm, emission wavelength: 521 nm for FL; excitation wavelength: 560 nm,

emission wavelength: 590 nm for RhB), using the PBS buffer solution as the blank sample. The calibration curves of FL and RhB are shown in Figure 5.3 and Figure 5.4.

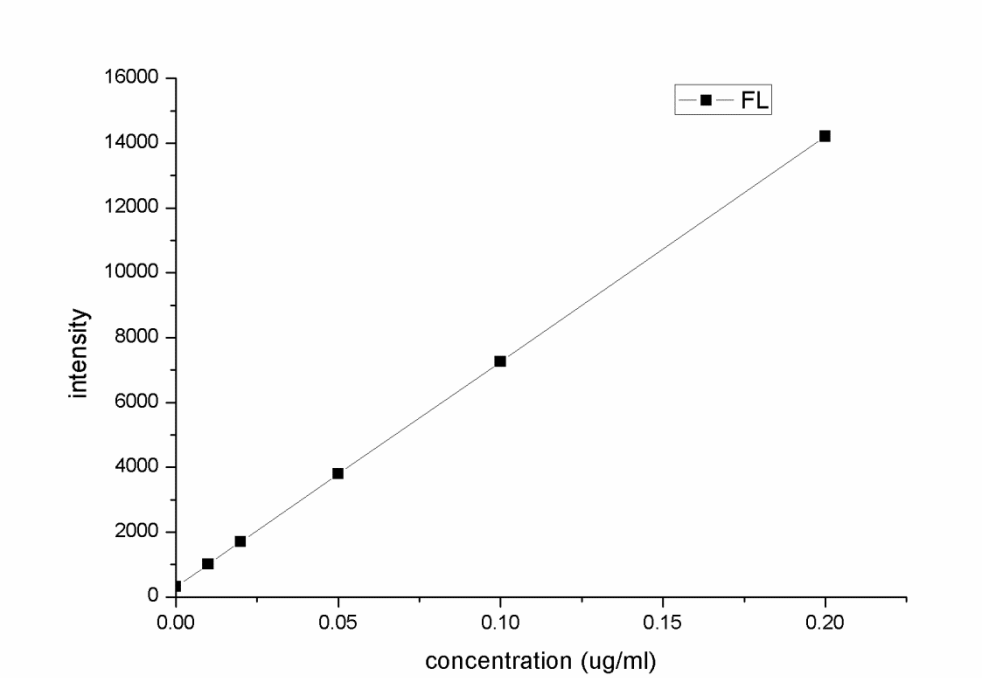

Figure 5.3 Standard curve of FL in PBS buffer solution

The equation of the curve is: I=69453C+311 with the correlation coefficient of 0.9998, where I and C denote the intensity of fluorescence and the concentration of FL, respectively.

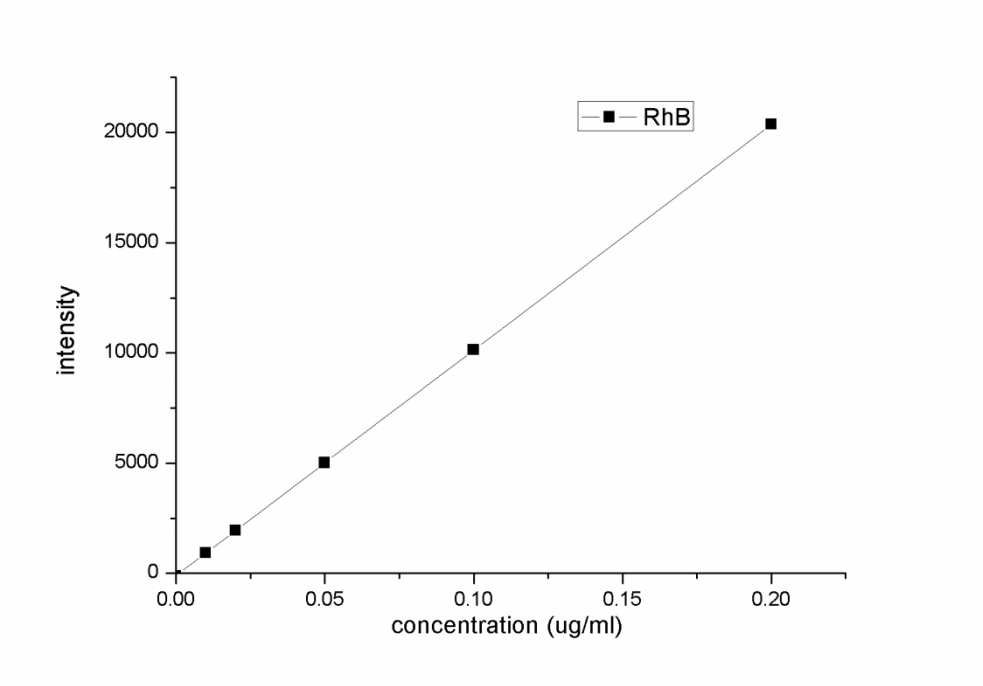

Figure 5.4 Standard curve of RhB in PBS buffer solution

The equation of the curve is: I=102350C-109 with the correlation coefficient of 0.9987, where I and C denote the intensity of fluorescence and the concentration of RhB, respectively.

5.3.5 Drug release quantification and data analysis

This section is similar to section 4.3.8 and 4.3.9, with the only difference of using the PBS buffer solution as the blank sample.

5.4 Results and Discussion

5.4.1 Effect of length of agarose gel on the release profiles

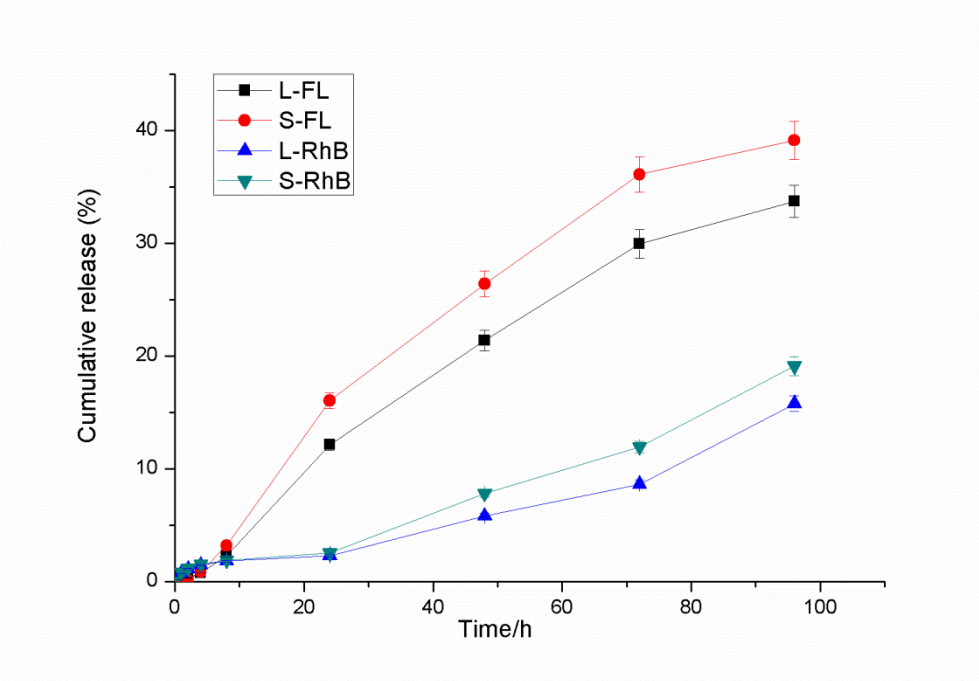

Figure 5.5 Effect of length of agarose gel on the release profiles of FL and RhB at 37 ℃

The effect of length of agarose gel on the release profiles was shown in Figure 5.5. By the comparison between L-FL and S-FL or between L-RhB and S-RhB, it could be concluded that with the increase of the length of agarose gel, the release rate of drug from the upper layer or lower layer was decreased. It could be attributed to the difference of drug diffusion rate through the rod of agarose gel. Therefore, according to the different

requirement of drugs loaded in the multi-drug delivery tube, it is easy to meet the needs just by adjusting the length of each agarose gel.

In addition, from the figure we also can see, both FL and RhB showed a sustained release profile, while the release rate of FL (the upper layer of gelatin gel) was faster than that of RhB (the lower layer of gelatin gel), which estimated that with the different depth of drug-loaded gelatin layer, the drug release rate was different. Therefore, multi-layers of different drug-loaded gelatin gel could be prepared in this multi-drug delivery tube for multi-drug delivery with different release profiles.

5.4.2 Effect of temperature on the release profiles

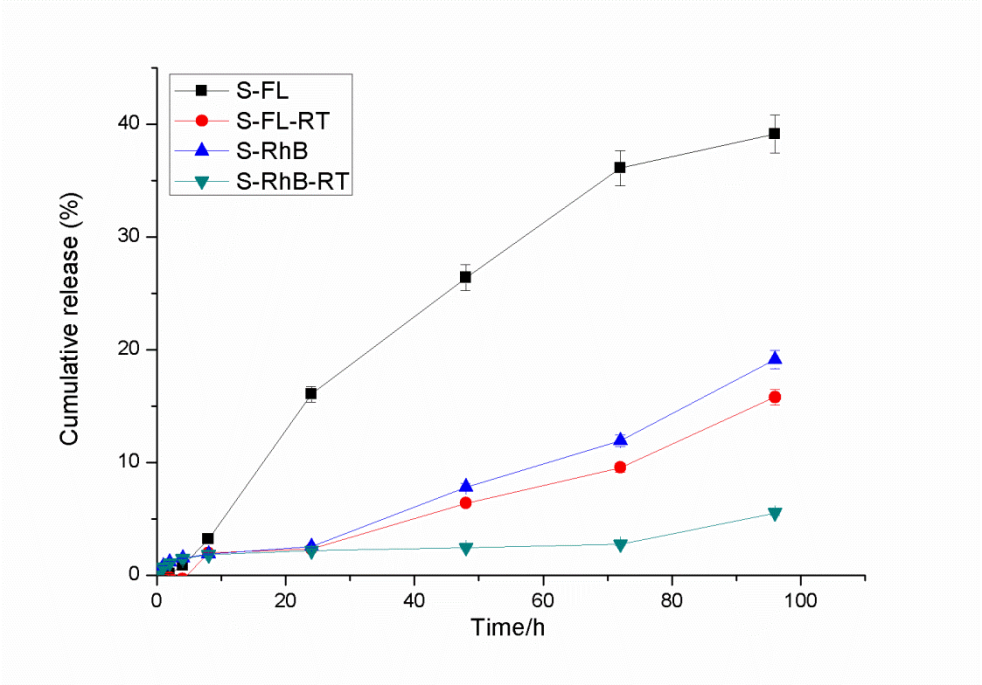

Figure 5.6 Effect of temperature on the release profiles of FL and RhB with 1 cm-length agarose gel

The effect of temperature on the release profiles was presented in Figure 5.6. The significant difference between the release profiles at RT and 37 ℃ could be observed, no matter FL or RhB. As a matter of fact, gelatin gel was still in solid state when the multi-drug delivery system was placed at RT, it is quite difficult for the molecules of drugs to diffuse through solid gel; while gelatin gel would melt when placed at 37 ℃, which would accelerate the diffusion of drugs from melted gelatin solution.

5.5 Conclusions

A novel and simple model of multi-drug delivery system was designed and fabricated by putting the rods of agarose gel and drug-loaded gelatin gel into a polycarbonate tube layer by layer. The gelatin-drug conjugate (chapter 3 and 4) was still the key factor in this system. The length of diffusion barriers (agarose gel) and temperature had great influence on the release profiles of both drugs, no matter in upper gelatin layer or in lower gelatin layer. Operating in a similar way, multiple drugs could be loaded into gelatin gel separated by agarose layers. However, this chapter just provides an idea for multi-drug delivery system, more effort to put this system into practical application is worthwhile, especially in the aspects of the dimension and material of the device (tube and membrane). As for the dimension, it should be suitable for the practical application (ultimately in vivo), micro-sized or millimeter-sized is preferable. And as for the material, it should be biodegradable and biocompatible, at least, non-toxic to the body, like titania nanotube, already used by Moom [126].

Chapter 6

Final Remarks

6.1 Conclusions

This thesis investigated the production of drug delivery system based on the uncross-linked gelatin. The main results are as following:

First, based on the study of all the preparation parameters, the optimal condition for the preparation of gelatin microbeads is: 100 μg/mL (10%) gelatin solutions, 1: 5 of water/oil volume ratio, 10 min of emulsifying time and 800 rpm of the stirring speed.

Then, a novel drug delivery system consisting of drug-loaded uncross-linked gelatin microbeads and cross-linkable alginate matrix was fabricated. The drug release profile was studied, which showed a drastic reduction of initial burst release and a sustained release up to 200 hours by the synergistic interplay between gelatin and drug. Release profile can be easily modulated by varying drug-loading concentration in the gelatin microbeads, the alginate-to-gelatin ratio, and temperature.

In addition, a dual-drug delivery system based on the chapter 3 was prepared and the release profiles of two drugs were investigated. The dual-drug release test in vitro showed a fast release for FL loaded in alginate and a sustained release for RhB loaded in gelatin microbeads.

Finally, an idea for the multi-drug delivery system was demonstrated by putting the rods of agarose gel and drug-loaded gelatin gel into a polycarbonate tube layer by layer. With the increase of the length of agarose gel or decrease of the temperature, release profiles of all the drugs could be declined. Multiple drugs could be loaded in different layers of gelatin gel.

6.2 Future Work

In this thesis, the model drugs we used are kind of dyes, not real drugs, it is better to transfer the drug delivery system to the practical application by using the real drugs. As for the fifth chapter, the suitable dimension and materials of the device also should be considered to improve.

Bibliography

1. Kumari, A., S.K. Yadav, and S.C. Yadav, *Biodegradable polymeric nanoparticles based drug delivery systems.* Colloids and Surfaces B: Biointerfaces, 2010. **75**(1): p. 1-18.
2. Ko, J.A., et al., *Preparation and characterization of chitosan microparticles intended for controlled drug delivery.* International Journal of Pharmaceutics, 2002. **249**(1–2): p. 165-174.
3. Ravi Kumar, M.N.V., U. Bakowsky, and C.M. Lehr, *Preparation and characterization of cationic PLGA nanospheres as DNA carriers.* Biomaterials, 2004. **25**(10): p. 1771-7.
4. Allen, T.M. and P.R. Cullis, *Drug delivery systems: Entering the mainstream.* Science, 2004. **303**: p. 1818-1822.
5. Qiu, Y. and K. Park, *Environment-sensitive hydrogels for drug delivery.* Advanced Drug Delivery Reviews, 2012. **64**: p. 49-60.
6. Zhang, Y., H.F. Chan, and K.W. Leong, *Advanced materials and processing for drug delivery: The past and the future.* Adv. Drug Deliv. Rev, 2013. **65**(1): p. 104-120.
7. Verma, R.K.G., *Current status of drug delivery technologies and future directions.* Pharm. Technol, 2001. **25**: p. 1-14.

8. Almeida, A.J. and E. Souto, *Solid lipid nanoparticles as a drug delivery system for peptides and proteins.* Adv. Drug Deliv. Rev, 2007. **59**: p. 478-490.
9. Zhang, L., et al., *Development of nanoparticles for antimicrobial drug delivery.* Curr. Med. Chem, 2010. **17**: p. 585-594.
10. Bertrand, N. and J.-C. Leroux, *The journey of a drug-carrier in the body: An anatomo-physiological perspective.* Journal of Controlled Release, 2012. **161**(2): p. 152-163.
11. Wang, N.X. and H.A. von Recum, *Affinity-Based Drug Delivery.* Macromolecular Bioscience, 2011. **11**(3): p. 321-332.
12. Arifin, D.Y., L.Y. Lee, and C.-H. Wang, *Mathematical modeling and simulation of drug release from microspheres: Implications to drug delivery systems.* Advanced Drug Delivery Reviews, 2006. **58**: p. 1274-1325.
13. Liew, C.V., et al., *Evaluation of sodium alginate as drug release modifier in matrix tablets.* International Journal of Pharmaceutics, 2006. **309**(1-2): p. 25-37.
14. Oupicky, D., et al., *Stimulus-controlled delivery of drugs and genes.* Expert Opin. Drug Delivery, 2005. **2**: p. 653-665.
15. Alarcon, C.d.l.H., S. Pennadam, and C. Alexander, *Stimuli responsive polymers for biomedical applications.* Chemical Society Reviews, 2005. **34**(3): p. 276-285.
16. Peppas, N.A., et al., *Physicochemical, foundations and structural design of hydrogels in medicine and biology.* Annual Review of Biomedical Engineering, 2000. **2**: p. 9-29.

17. Brazel, C.S. and N.A. Peppas, *Modeling of drug release from swellable polymers.* European Journal of Pharmaceutics and Biopharmaceutics, 2000. **49**(1): p. 47-58.
18. Siepmann, J. and A. Gopferich, *Mathematical modeling of bioerodible, polymeric drug delivery systems.* Advanced Drug Delivery Reviews, 2001. **48**(2-3): p. 229-247.
19. Tabata, Y. and Y. Ikada, *Protein release from gelatin matrices.* Adv. Drug Deliv. Rev, 1998. **31**: p. 287-301.
20. Schipper, M.L., et al., *Particle size, surface coating, and PEGylation influence the biodistribution of quantum dots in living mice.* Small, 2009. **5**: p. 126-134.
21. Carrstensen, H., R.H. Muller, and B.W. Muller, *Particle size, surface hydrophobicity and interaction with serum of parenteral fat emulsions and model drug carriers as parameters related to RES uptake.* Clin. Nutr, 1992. **11**: p. 289-297.
22. Cabral, H., et al., *Accumulation of sub-100 nm polymeric micelles in poorly permeable tumours depends on size.* Nat. Nanotechnol, 2011. **6**: p. 815-823.
23. Jain, R., et al., *Controlled drug delivery by biodegradable poly(ester) devices: different preparative approaches.* Drug Dev. Ind. Pharm, 1998. **24**: p. 703-727.
24. Jain, R.A., *The manufacturing techniques of various drug loaded biodegradable poly(lactide-co-glycolide) (PLGA) devices.* Biomaterials, 2000. **21**: p. 2475-2490.
25. A.S. Hoffman, *The origins and evolution of "controlled" drug delivery systems.* Journal of Controlled Release, 2008. **132**: p. 153-163.

26. Schrieber, R. and H. Gareis, eds. *Gelatine handbook*. 2007, Wiley-VCH: Weinheim.
27. Lee, E.J., et al., *Studies on the characteristics of drug-loaded gelatin nanoparticles prepared by nanoprecipitation.* Bioprocess and Biosystems Engineering, 2011. **35**(1-2): p. 297-307.
28. Wade A, W.P., ed. *Hand book of pharmaceutical excipients, 2nd edn*. 1995, Pharmaceutical Press: London.
29. Migliaresi, C., et al., *Therapeutic use of gelatin hydrogels with a gel-sol transition at body temperature*. 2013: Italy patent WO2013045689 A1.
30. Fu, Y., et al., *3D cell entrapment in crosslinked thiolated gelatin-poly(ethylene glycol) diacrylate hydrogels.* Biomaterials, 2012. **33**(1): p. 48-58.
31. Lee, E.J., et al., *Studies on the characteristics of drug-loaded gelatin nanoparticles prepared by nanoprecipitation.* Bioprocess and Biosystems Engineering, 2012. **35**(1-2): p. 297-307.
32. Tabata, Y. and Y. Ikada, *Protein release from gelatin matrices.* Advanced Drug Delivery Reviews, 1998. **31**(3): p. 287-301.
33. Veis, A., ed. *The Macromolecular Chemistry of Gelatin*. 1964, Academic Press: New York.
34. Amini, A.A. and L.S. Nair, *Enzymatically cross-linked injectable gelatin gel as osteoblast delivery vehicle.* Journal Of Bioactive and Compatible Polymers, 2012. **27**(4): p. 342-355.
35. Lee, E.J., et al., *Studies on the characteristics of drug-loaded gelatin nanoparticles prepared by nanoprecipitation.* Bioprocess and Biosystems Engineering, 2012. **35**(1-2): p. 297-307.

36. Kumari, A., S.K. Yadav, and S.C. Yadav, *Biodegradable polymeric nanoparticles based drug delivery systems.* Colloids and Surfaces B-Biointerfaces, 2010. **75**(1): p. 1-18.
37. Wu, S.C., et al., *Cell adhesion and proliferation enhancement by gelatin nanofiber scaffolds.* Journal Of Bioactive and Compatible Polymers, 2011. **26**(6): p. 565-577.
38. Xiao, W., et al., *Ultrasonication and Genipin Cross-Linking to Prepare Novel Silk Fibroin-Gelatin Composite Hydrogel.* Journal Of Bioactive and Compatible Polymers, 2012. **27**(4): p. 327-341.
39. Dong, Z., Q. Wang, and Y. Du, *Alginate/gelatin blend films and their properties for drug controlled release.* Journal Of Membrane Science, 2006. **280**(1-2): p. 37-44.
40. Liao, I.C., et al., *Controlled release from fibers of polyelectrolyte complexes.* Journal Of Controlled Release, 2005. **104**(2): p. 347-358.
41. Balakrishnan, B. and A. Jayakrishnan, *Self-cross-linking biopolymers as injectable in situ forming biodegradable scaffolds.* Biomaterials, 2005. **26**(18): p. 3941-3951.
42. Ofner, C.M., et al., *Growth inhibition, drug load, and degradation studies of gelatin/methotrexate conjugates.* International Journal of Pharmaceutics, 2006. **308**(1-2): p. 90-99.
43. Stehle, G., et al., *The loading rate determines tumor targeting properties of methotrexate-albumin conjugates in rats.* Anti-Cancer Drugs, 1997. **8**(7): p. 677-85.
44. Smidsrod, O. and G. Skjak-Braek, *Alginate as immobilization matrix for cells.* TIBTECH, 1990. **8**: p. 71-78.
45. Sutherland, I.W., ed. *Alginates*. Biomaterials; Novel Materials from Biological Sources, ed. D. Byrom. 1991, Stockton: New York.

46. MacGregor, E.A. and C.T. Greenwood, eds. *Polymers in Nature in Polysaccharides*. 1980, Wiley: New York.
47. Drury, J.L. and D.J. Mooney, *Hydrogels for tissue engineering: scaffold design variables and applications.* Biomaterials, 2003. **24**(24): p. 4337-4351.
48. Rowley, J.A., G. Madlambayan, and D.J. Mooney, *Alginate hydrogels as synthetic extracellular matrix materials.* Biomaterials, 1999. **20**(1): p. 45-53.
49. Gombotz, W.R. and S.F. Wee, *Protein release from alginate matrices.* Advanced Drug Delivery Reviews, 2012. **64**: p. 194-205.
50. Byrom, D., ed. *Biomaterials: Novel Materials from Biological Sources*. Alginates, ed. I.W. Sutherland. 1991, Stockton: New York. 309-331.
51. Clark, A.H. and S.B. Ross-Murphy, *Structural and mechanical properties of biopolymer gels.* Adv. Polym. Sci, 1987. **83**: p. 57-192.
52. Smidsrod, O. and G. Skjakbraek, *Alginate as immobilization matrix for cells.* Trends in Biotechnology, 1990. **8**(3): p. 71-78.
53. Hori, Y., A.M. Winans, and D.J. Irvine, *Modular injectable matrices based on alginate solution/microsphere mixtures that gel in situ and co-deliver immunomodulatory factors.* Acta Biomaterialia, 2009. **5**(4): p. 969-982.
54. Kandalam, U., et al., *Viability of human umbilical cord-derived mesenchymal stem cells in G-rich and M-rich alginates.* Journal Of Bioactive and Compatible Polymers, 2012. **27**(2): p. 174-182.
55. Goh, C.H., P.W.S. Heng, and L.W. Chan, *Alginates as a useful natural polymer for microencapsulation and therapeutic applications.* Carbohydrate Polymers, 2012. **88**(1): p. 1–12.

56. Bhushan, I. and R. Parshad, *Immobilization of lipase by entrapment in Ca-alginate beads.* J Bioact Compat Pol 2008. **23**(6): p. 552-562.
57. Gasperini, L., D. Maniglio, and C. Migliaresi, *Microencapsulation of cells in alginate through an electrohydrodynamic process.* Journal Of Bioactive and Compatible Polymers, 2013. **28**(5): p. 413-425.
58. Jejurikar, A., et al., *Degradable alginate hydrogels crosslinked by the macromolecular crosslinker alginate dialdehyde.* Journal Of Materials Chemistry, 2012. **22**(19): p. 9751.
59. Kuo, C.K. and P.X. Ma, *Ionically crosslinked alginate hydrogels as scaffolds for tissue engineering: Part 1. Structure, gelation rate and mechanical properties.* Biomaterials, 2001. **22**(6): p. 511-521.
60. Bai, X., et al., *Self-cross-linkable hydrogels composed of partially oxidized alginate and gelatin for myocardial infarction repair.* Journal of Bioactive and Compatible Polymers, 2013. **28**(2): p. 126-140.
61. Ito, T., et al., *Preparation of injectable auto-forming alginate gel containing simvastatin with amorphous calcium phosphate as a controlled release medium and their therapeutic effect in osteoporosis model rat.* Journal of Materials Science: Materials in Medicine, 2012. **23**(5): p. 1291-1297.
62. Cohen, S., et al., *A novel in situ-forming opthalmic drug delivery system from alginates undergoing gelation in the eye.* J. Control. Release, 1997. **44**: p. 201-208.
63. Kwok, K.K., M.J. Groves, and D.J. Burgess, *Production of 5 - 15 μm diameter alginate-polylysine microcapsules by air-atomization technique.* Pharm. Res., 1991. **8**: p. 341-344.

64. Hara, M., *Polyelectrolytes: Science and Technology*. 1993, Marcel Dekker: New York.
65. Duvvuri, S., K. Janoria, and A. Mitra, *Development of a novel formulation containing poly(D,L-lactide-co-glycolide) microspheres dispersed in PLGA–PEG–PLGA gel for sustained delivery of ganciclovir.* Journal of Controlled Release, 2005. **108**(2-3): p. 282-293.
66. Zhong, D.G., et al., *Study on poly(D,L-lactic) microspheres embedded in calcium alginate hydrogel beads as dual drug delivery systems.* Journal of Applied Polymer Science, 2013. **129**(2): p. 767-772.
67. Wei, L., et al., *Dual-drug delivery system based on hydrogel/micelle composites.* Biomaterials, 2009. **30**(13): p. 2606-2613.
68. Mandal, B.B. and S.C. Kundu, *Calcium alginate beads embedded in silk fibroin as 3D dual drug releasing scaffolds.* Biomaterials, 2009. **30**(28): p. 5170-5177.
69. Xu, J., et al., *Controlled dual release of hydrophobic and hydrophilic drugs from electrospun poly(l-lactic acid) fiber mats loaded with chitosan microspheres.* Materials Letters, 2011. **65**(17-18): p. 2800-2803.
70. Esposito, E., R. Cortesi, and C. Nastruzzi, *Gelatin microspheres: influence of preparation parameters and thermal treatment on chemico-physical and biopharmaceutical properties.* Biomaterials, 1996. **17**: p. 2009-2020.
71. Lee, K., et al., *Monoclonal antibody-based targeting of methotrexate-loaded microspheres.* Int J Pharm, 1990. **59**: p. 27-33.

72. Tomlinson, E., ed. *Drug Delivery Systems. Fundamentals and Techniques*. Biological opportunities for site-specific drug delivery using particulate carriers. 1987, Ellis Horwood Ltd: Chichester.
73. Zhang, Y., H.F. Chan, and K.W. Leong, *Advanced materials and processing for drug delivery: The past and the future.* Advanced Drug Delivery Reviews, 2013. **65**(1): p. 104-120.
74. Shenoy, D.B. and M.M. Amiji, *Poly(ethylene oxide)-modified poly(epsilon-caprolactone) nanoparticles for targeted delivery of tamoxifen in breast cancer.* Int. J. Pharm, 2006. **293**: p. 261-270.
75. Schroeder, U., et al., *Nanoparticle technology for delivery of drugs across the blood–brain barrier*. J. Pharm. Sci, 1998. **87**(11): p. 1305-1307.
76. Alexis, F., et al., *Factors affecting the clearance and biodistribution of polymeric nanoparticles.* MOl. Pharm, 2008. **5**(4): p. 505-515.
77. Budhian, A., S.J. Siegel, and K.I. Winey, *Production of haloperidol-loaded PLGA nanoparticles for extended controlled drug release of haloperidol.* J. Microencapsul, 2005. **22**(7): p. 773-785.
78. Mu, L. and S.S. Feng, *A novel controlled release formulation for the anticancer drug paclitaxel (Taxol): PLGA nanoparticles containing vitamin E TPGS.* J. Control. Release, 2003. **86**(1): p. 33-48.
79. Damge, C., P. Maincent, and Ubrich, *Oral delivery of insulin associated to polymeric nanoparticles in diabetic rats.* J. Control. Release, 2007. **117**(2): p. 163-170.
80. Date, A.A., M.D. Joshi, and V.B. Patravale, *Parasitic diseases: liposomes and polymeric nanoparticles versus lipid nanoparticles.* Advanced Drug Delivery Reviews, 2007. **59**(6): p. 505-521.

81. Kim, S.Y. and Y.M. Lee, *Taxol-loaded block copolymer nanospheres composed of methoxy poly(ethylene glycol) and poly(epsilon-caprolactone) as novel anticancer drug carriers.* Biomaterials, 2001. **22**(13): p. 1697-1704.
82. Kohane, D.S., et al., *Effectiveness of muscimol-containing microparticles against pilocarpine-induced focal seizures.* Epilepsia, 2002. **43**(12): p. 1462-1468.
83. Kohane, D.S., et al., *Biodegradable polymeric microspheres and nanospheres for drug delivery in the peritoneum.* J Biomed Mater Res A, 2006. **77**(2): p. 351-361.
84. Elisabetta, E., C. Rita, and N. Claudio, *Gelatin microspheres influence of preparation parameters and thermal treatment on chemico-physical and biopharmaceutical properties.* Biomaterials 1996. **17**(20): p. 2009-2020.
85. RASSOUL, D., et al., *Preparation of gelatin microspheres containing lactic acid-effect of cross-linking on drug release.* Acta Pharma, 2005. **55**: p. 57-67.
86. Lemoine, D., et al., *Preparation and characterization of alginate microspheres containing a model antigen.* International Journal of Pharmaceutics, 1998. **176**(1): p. 9-19.
87. Oh, J.K., et al., *The development of microgels/nanogels for drug delivery applications.* Progress In Polymer Science, 2008. **33**(4): p. 448-477.
88. Tanaka, N., S. Takino, and I. Utsumi, *A new oral gelatinized sustained-release dosage form.* Journal Of Pharmaceutical Sciences, 1963. **52**(7): p. 664-667.

89. Khalid, N., et al., *Preparation and Characterization of Water-in-Oil-in-Water Emulsions Containing a High Concentration of L-Ascorbic Acid.* Bioscience, Biotechnology, and Biochemistry, 2013. **77**(6): p. 1171-1178.
90. Freiberg, S. and X.X. Zhu, *Polymer microspheres for controlled drug release.* INT J Pharm, 2004. **282**: p. 1-18.
91. Yu, L. and J. Ding, *Injectable hydrogels as unique biomedical materials.* Chem Soc Rev, 2008. **37**(8): p. 1473-1481.
92. Lee, K.Y. and D.J. Mooney, *Hydrogels for tissue engineering.* Chem Rev, 2001. **101**(7): p. 1869-1879.
93. Bae, K.H., L.S. Wang, and K. Motoichi, *Injectable biodegradable hydrogels: progress and challenges.* J. Mater. Chem. B, 2013. **1**(40): p. 5371-5388.
94. He, C.L., S.W. Kim, and D.S. Lee, *In situ gelling stimuli-sensitive block copolymer hydrogels for drug delivery.* J Control Release, 2008. **127**(3): p. 189-207.
95. Wang, F., et al., *Injectable, rapid gelling and highly flexible hydrogel composites as growth factor and cell carriers.* Acta Biomaterialia, 2010. **6**(6): p. 1978-1991.
96. Jeong, B., et al., *Biodegradable block copolymers as injectable drug-delivery systems.* Nature, 1997. **388**(6645): p. 860-862.
97. Gong, C.Y., et al., *Biodegradable in situ gel-forming controlled drug delivery system based on thermosensitive PCL–PEG–PCL hydrogel. Part 2: Sol–gel–sol transition and drug delivery behavior.* Acta Biomaterialia, 2009. **5**(9): p. 3358-3370.

98. Zentner, G.M., et al., *Biodegradable block copolymers for delivery of proteins and water-insoluble drugs.* Journal of Controlled Release, 2001. **72**(1-3): p. 203-215.
99. Gong, C., et al., *Synthesis and characterization of PEG-PCL-PEG thermosensitive hydrogel.* International Journal of Pharmaceutics, 2009. **365**(1-2): p. 89-99.
100. Yuan, Y., et al., *The effect of cross-linking of chitosan microspheres with genipin on protein release.* Carbohydr.Polym, 2007. **68**: p. 561-567.
101. Tan, H., et al., *Gelatin/chitosan/hyaluronan scaffold integrated with PLGA microspheres for cartilage tissue engineering.* Acta Biomaterialia, 2009. **5**: p. 328-337.
102. Huang, Y., et al., *In vitro characterization of chitosan-gelatin scaffolds for tissue engineering.* Biomaterials, 2005. **26**: p. 7616-7627.
103. Nguyen, M.K. and D.S. Lee, *Injectable biodegradable Hydrogels.* Macromol Bioscience, 2010. **10**: p. 563-579.
104. Patel, R.B., et al., *Effect of injection site on in situ implant formation and drug release in vivo.* Journal Of Controlled Release, 2010. **147**(3): p. 350-358.
105. Alonso, M., et al., *Determinants of Release Rate of Tetanus Vaccine from Polyester Microspheres.* Pharmaceutical Research, 1993. **10**(7): p. 945-953.
106. Deng, X.M., et al., *Optimization of preparative conditions for poly-DL-lactide-polyethylene glycol microspheres with entrapped Vibrio Cholera antigens.* Journal of Controlled Release, 1999. **58**(2): p. 123-131.

107. Raja Mohd Hafidz, R., et al., *Chemical and functional properties of bovine and porcine skin gelatin.* International Food Research Journal 2011. **18**: p. 813-817.
108. Wade, A. and P.J. Weller, eds. *Handbook of pharmaceutical excipients, 2nd edn*. 1994, Pharmaceutical Press: London.
109. Allen, T.M., *Drug Delivery Systems: Entering the Mainstream.* Science, 2004. **303**(5665): p. 1818-1822.
110. Vallet-Reg ́ı M., et al., *Bone-regenerative bioceramic implants with drug and protein controlled delivery capability.* Prog. Solid State Chem., 2008. **36**: p. 163-191.
111. Tran, P.A., et al., *Opportunities for nanotechnology-enabled bioactive bone implants.* J. Mater. Chem., 2009. **19**: p. 2653-2659.
112. Porter, J.R., T.T. Ruckh, and K.C. Popat, *Bone tissue engineering: A review in bone biomimetics and drug delivery strategies.* Biotechnol. Prog., 2009. **25**(6): p. 1539-1560.
113. Qiu, L.Y. and Y.H. Bae, *Self-assembled polyethylenimine-graft-poly(ε-caprolactone) micelles as potential dual carriers of genes and anticancer drugs.* Biomaterials, 2007. **28**(28): p. 4132-4142.
114. Lee, J.S., et al., *Controlled dual release of basic fibroblast growth factor and indomethacin from heparin-conjugated polymeric micelle.* International Journal of Pharmaceutics, 2008. **346**(1-2): p. 57-63.
115. Lee, B.J., S.G. Ryu, and J.H. Cui, *Controlled release of dual drug-loaded hydroxypropyl methylcellulose matrix tablet using drug-containing polymeric coatings.* International Journal of Pharmaceutics, 1999. **188**(1): p. 71-80.

116. Qian, Q., et al., *Modulating the release of drugs from alginate matrices with the addition of gelatin microbeads.* Journal of Bioactive and Compatible Polymers, 2014. **29**(3): p. 193-207.
117. Choi, S.-W., Y. Zhang, and Y. Xia, *A Temperature-Sensitive Drug Release System Based on Phase-Change Materials.* Angewandte Chemie International Edition, 2010. **49**(43): p. 7904-7908.
118. Ruan, G. and S.S. Feng, *Preparation and characterization of poly(lactic acid)-poly(ethylene glycol)-poly(lactic acid) (PLA-PEG-PLA)microspheres for controlled release of paclitaxel.* Biomaterials, 2003. **24**(27): p. 5037-5044.
119. Patel, R.V. and M.M. Amiji, *Preparation and characterization of freeze-dried chitosan-poly(ethylene oxide) hydrogels for site-specific antibiotic delivery in the stomach.* Pharmaceutical Research, 1996. **13**(4): p. 588-593.
120. Almeida, P.F. and A.J. Almeida, *Cross-linked alginate–gelatine beads: a new matrix for controlled release of pindolol.* Journal Of Controlled Release, 2004. **97**(3): p. 431-439.
121. Langer, R., *Drugs on target.* Science, 2001. **293**: p. 58-59.
122. Acton, A.L., et al., *Janus PEG-Based Dendrimers for Use in Combination Therapy: Controlled Multi-Drug Loading and Sequential Release.* Biomacromolecules, 2013. **14**(2): p. 564-574.
123. Duncan, R., *The dawning era of polymer therapeutics.* Nat Rev Drug Discov, 2003. **2**(5): p. 347-360.
124. Harries, M. and M. Gore, *Chemotherapy for epithelial ovarian cancer treatment as first diagnosis.* Lancet Oncol, 2002. **3**: p. 529-536.

125. Reich, S., et al., *Low-dose chemotherapy with vinblastine and methotrexate in childhood desmoid tumors.* J Clin Oncol, 1999. **17**: p. 1086.
126. Aw, M., J. Addai-Mensah, and D. Losic, *A multi-drug delivery system with sequential release using titania nanotube arrays.* Chem. Commun., 2012. **48**: p. 3348-3350.